EFFECTS OF ULTRASOUND EXPOSURE TO CELLS CULTURED ON NITINOL IN A PDMS SUBSTRATE

by

Cansu Şen

B.S., in Electrical and Electronics Engineering, Istanbul Bilgi University, 2017

Submitted to the Institute of Biomedical Engineering
in partial fulfillment of the requirements
for the degree of
Master of Science
in
Biomedical Engineering

Boğaziçi University
2021

ACKNOWLEDGMENTS

I would like to express my gratitude to people who have contributed to this work and have made this thesis possible.

Family comes first. I am very thankful to my parents and my little sister for their endless support. They always encourage me throughout my life. I know they will always stand by me. Love them so much.

My supervisor, Assoc. Prof. Özgür Kocatürk, gave me an opportunity to work with him. I am very grateful to him for his guidance and advices during my studies.

I also thank Assoc. Prof. Dr. Bora Garipcan for providing me the opportunity to work in the cell culture laboratory.

I am very thankful to Fatma Gülden Şimşek for her valuable contributions and ideas. She was always there when I needed. It could not be possible to finish this thesis without her support.

I warmly thank Seda Tarhan. She has always helped me every time when I was in a difficult situation.

There are some dearest people that I would like to mention here. My BME family; Bengü Aktaş, Hayriye Öztatlı, Morteza Teymoori, Sezin Eren, Meltem Uçar, Ecem Sakallı, Hasan Şahin, Kübra Gökmen, and Elif Dönmez. I deeply thank all of them for their valuable friendship.

I am very delighted work with my colleagues, Ayça Atay, Fırat Çakmak and Taha Hasekioğlu. Their support has made everything easier for me during this process.

I should also thank Oğuz Kaan Erden for keeping me motivated to complete this thesis and helping me whenever I need.

My lovely homemate, Selin Oturaklı, thank you for your precious support and endless patience during that time. And my beloved sisters, I always feel all of you being on my side since 2008.

ACADEMIC ETHICS AND INTEGRITY STATEMENT

I, Cansu Şen, hereby certify that I am aware of the Academic Ethics and Integrity Policy issued by the Council of Higher Education (YÖK) and I fully acknowledge all the consequences due to its violation by plagiarism or any other way.

Name :

Signature:

Date:

ABSTRACT

EFFECTS OF ULTRASOUND EXPOSURE TO CELLS CULTURED ON NITINOL IN A PDMS SUBSTRATE

Cardiovascular diseases (CVD) are one of the most serious health problems in the world. Especially atherosclerosis has a great influence on a heart attack. As a remedy, vascular stents are frequently used to prevent restenosis. It is very crucial to prohibit the smooth muscle cells growth not to generate any thrombus formation and to achieve endothelization on the stent surface. Therefore, some innovative, user-friendly, and non-invasive treatment methods such as ultrasound can be applied to the target tissue during and after the implantation surgery. In this thesis, L929 mouse fibroblast cells and MCF-7 (Michigan Cancer Foundation-7) human breast cancer cells have been chosen to evaluate the ultrasound effect. While ultrasound exposure has been utilized to observe the cellular viability of fibroblast cells, it has been applied to breast cancer cells to bring cell proliferation under control and/or see cell necrosis. Since ultrasound has provided both the endothelization and preventing the smooth muscle cell generation leading to vessel occlusion, this in-vitro study can be the representative solution for in-stent restenosis regarding the impact of ultrasound for both cells generation and/or cell necrosis. Also, these cell lines have been cultured on Nitinol (NiTi) surfaces placed into the PDMS substrates to represent the NiTi-based stent in the vessel structure. Based on our results, the highest viability of fibroblast cells was detected at low intensities; 0.2 W/cm^2, 1 MHz, and 0.2 W/cm^2, 3 MHz. Moreover, for MCF-7 cells, there has been no statistically significant difference in cell proliferation following ultrasound exposure. Therefore, it can be claimed that ultrasound treatment can aid to control cancer cell generation on NiTi surfaces. Consequently, it might be a prospective and promising study to explore the influence of ultrasound on both endothelization and to prohibit any obstruction in the vessel, which causes atherosclerosis.

ÖZET

PDMS'E YERLEŞTİRİLEN NİTİNOL ÜZERİNE KÜLTÜRLENEN HÜCRELERE ULTRASON UYGULAMASININ ETKİLERİ

Kardiyovasküler hastalıklar dünyadaki en ciddi sağlık sorunlarından biridir. Özellikle aterosklerozun kalp krizi üzerinde büyük etkisi vardır. Bu duruma çözüm niteliğinde, restenozu önlemek için vasküler stentler sıklıkla kullanılır. Düz kas hücrelerinin büyümesini engellemek, trombüs oluşturmamak ve stent yüzeyinde endotelizasyon sağlamak için çok önemlidir. Bu nedenle implantasyon ameliyatı sırasında ve sonrasında hedef dokuya ultrason gibi yenilikçi, kullanıcı dostu ve non-invaziv tedavi yöntemleri uygulanabilmektedir. Bu tezde, ultrason etkisini değerlendirmek için L929 fare fibroblast hücreleri ve MCF-7 (Michigan Cancer Foundation-7) insan meme kanseri hücreleri seçilmiştir. Ultrason uygulaması, fibroblast hücrelerinin hücresel canlılığını gözlemlemek için kullanılırken, hücre proliferasyonunu kontrol altına almak ve/veya hücre nekrozunu görmek için meme kanseri hücrelerine uygulanmıştır. Ultrason hem endotelizasyon sağladığından hem de damar tıkanıklığına yol açan düz kas hücresi oluşumunu engellediğinden, bu in vitro çalışma, ultrasonun hem hücre oluşumu hem de hücre nekrozu üzerindeki etkisine ilişkin olarak stent içi restenoz için temsili bir çözüm olabilir. Ayrıca, bu hücre hatları, damar yapısındaki NiTi bazlı stenti temsil etmek için PDMS substratlarına yerleştirilen NiTi yüzeyleri üzerinde kültürlenmiştir. Sonuçlarımıza göre, fibroblast hücrelerinin en yüksek canlılığı, düşük yoğunluklarda saptandı; 0,2 W/cm^2, 1 MHz ve 0,2 W/cm^2, 3 MHz. Ayrıca, MCF-7 hücreleri için, ultrasona uygulamasının ardından hücre proliferasyonunda istatistiksel olarak anlamlı bir fark görülmemiştir. Bu nedenle, ultrason tedavisinin NiTi yüzeylerde kanser hücresi oluşumunu kontrol etmeye yardımcı olabileceği iddia edilebilir. Sonuç olarak, ultrasonun hem endotelizasyon üzerindeki etkisini araştırmak hem de damarda ateroskleroza neden olan herhangi bir tıkanıklığı önlemek için ileriye dönük ve umut verici bir çalışma olabilir.

TABLE OF CONTENTS

LIST OF FIGURES

LIST OF TABLES

LIST OF SYMBOLS

°C	Celcius

LIST OF ABBREVIATIONS

$3D$	Three Dimensional
AO	Acridine Orange
AB	Alamar Blue
Af	Austenite finish
As	Austenite start
$ATCC$	American Type of Culture Collection
BES	Balloon Expandable Stent
BMS	Bare Metal Stents
BRS	Bioresorbable Stent
BVS	Bioresorbable Vascular Scaffold
BSA	Bovine Serum Albumin
CO^2	Carbon dioxide
CVD	Cardiovascular Disease
CAS	Carotid Artery Stenting
$Co-Cr$	Cobalt-Chromium
$Co-Ni$	Cobalt-Nickel
CAD	Computer Aided Design
$DAPI$	4',6-diamidino-2-phenylindole
DNA	Deoxyribonucleic acid
DES	Drug-Eluting Stent
$DMEM$	Dulbecco's Modified Eagle's Medium
EtO	Ethylene Oxide
ECM	Extra Cellular Matrix
FBS	Fetal Bovine Serum
ISR	In-stent Restenosis
Fe	Iron
Mg	Magnesium
$Ni-Ti$	Nickel-Titanium

$REDOX$	Oxidation-reduction
PFA	Paraformaldehyde
PCI	Percutaneous Coronary Intervention
PTA	Percutaneous Transluminal Angioplasty
PAD	Peripheral Arterial Disease
PBS	Phosphate Buffered Saline
$Pt-Cr$	Platinum-Chromium
$Pt-Co$	Platinum-Cobalt
$Pt-Ir$	Platinum-Iridium
$PDMS$	Polydimethylsiloxane
PLA	Polylactide
$PTFE$	Polytetrafluoroethylene
PI	Propidium Iodide
$SEMS$	Self-Expandable Metal Stent
SMA	Shape-memory Alloy
SS	Stainless Steel
ST	Stent Thrombosis
Ta	Tantalum
TUS	Therapeutic Ultrasound
TCP	Tissue Culture Polystyrene
Ti	Titanium
WHO	World Health Organization

1. INTRODUCTION

Cardiovascular diseases (CVD) are the leading cause of mortality in Turkey and throughout the world in the twenty-first century [1–5] with atherosclerosis having the greatest incidence rate among cardiovascular diseases [6, 7], and vascular stents are usually preferred for the interventional treatment of atherosclerosis [8–12].

Atherosclerosis, or artery blockage, is the aggregation of some fibrous structure that includes smooth muscle cells [13] in the intima [7]. It is the leading reason of CVD such as myocardial and cerebral infections [7, 13, 14], angina pectoris, [4, 7], stroke [7,12–15], formation of aneurysms [7], intermittent claudication [7] due to the lesions composed of excessive amount of inflammatory and fibroproliferative reaction [13]. Thus, it remains one of the most prevalent reasons of death due to CVD [13–16]. As a solution, percutaneous coronary procedures are chosen instead of the conventional treatments such as conventional balloon angioplasty [12]. Nowadays, the most often used type of percutaneous intervention is stenting [5,12,17]. It is utilized in clinical purpose and has also been improved in the scientific community [5]. The primary objective of these scientific researches is to improve the design and biocompatibility of the vascular stents by enhancing its anti-thrombogenic, anti-restenotic, and endothelization characteristics [4, 5].

Stent manufacturing technology has evolved significantly over several decades by including different stent geometries, hybrid material specifications [18], and structure of the stent [11, 19], coating the stent with drugs [4, 10, 20–22] and drug-loaded polymer-stent systems [10] to avoid in-stent restenosis, stent thrombosis. However, those categories may not provide a certain solution to in-stent restenosis [19], which may emerge as a result of chronic infections linked to vascular damage during stent placement and/or owing to the patient's susceptible physiological circumstances.

There have been many studies investigated on the impact of ultrasonography

on cell viability. No research study could have been found conducted on the effect of iterative ultrasonic therapy on cell growth on the stent surface in the literature so far. The effects of low-intensity and low-frequency ultrasound on the viability of different cell lines on the stent surface, or the contributions of ultrasound waves to stent biocompatibility such as endothelial cell proliferation and prevention of smooth muscle cells not to generate in-stent restenosis, will be enquired in this thesis.

Ultrasound application for a therapeutic purpose is used for several biomedical applications because it can stimulate a localized target area in a cellular level. Also, different dosages can be applied sequentially to observe the ultrasound effect for the biological activity of the cell lines easily through in-vitro experiment setup.

To mimic the vessel structure, polydimethylsiloxane (PDMS) is a highly preferred biomaterial for cell culture due to its similarities to biological tissues in terms of properties such as elasticity, transparency, biocompatibility, and chemical stability in this thesis [23–26]. It is a hyper elastic material with a large modulus of elasticity, reducing the susceptibility to inflammation once implanted into the tissue [27].

Another highly biocompatible material Nitinol (NiTi), a nickel-titanium alloy is utilized to simulate the stent material in this thesis. NiTi alloys have unique properties such as shape memory and super-elastic properties thanks to its thermoelastic martensitic transformation. Since the transformation temperature of NiTi can be set to very close to the human body temperature, it is widely chosen biomaterial for many biomedical applications such as vascular guide wires [28,29], snares [29], self-expanding stents [28–31], heart valves [28], needles [30], occluders [29,30], arch wires of orthodontic braces [28,29], dental drills [30], inferior vena cava filters [29], anchor for orthopedic surgeries, and staples for the fixation of the bone fracture [29].

Despite the fact that research into the role of ultrasound in cell viability and proliferation is limited, there are many different current findings. There are research studies that demonstrate ultrasound promotes cell proliferation, but there are other studies that show it has no effect on it. Because of factors such as the experimental

design of the referenced research and the properties of the ultrasonic emitter used, the effect of ultrasound on cell viability has been interpreted in a variety of ways. That's why additional research studies are required to provide more specific information on this issue. New approaches should be tried to avoid in-stent restenosis and accelerate the endothelization process on the stent surface.

At this point, this thesis aims to observe the biological effect of ultrasound waves at different dosages on the particular cell lines; L929 mouse fibroblast cells and MCF-7 human breast cancer cells. Some of the studies in the past has investigated the ultrasound effect on the endothelial cells and the smooth muscle cells. When ultrasound was directly applied to the cell culture, it has contributed endothelial cell proliferation and to inhibit the smooth muscle cell generation to avoid in-stent restenosis. As a preliminary study, ultrasound waves have been applied to fibroblast cells which is the responsible of some physiological activities such as wound healing, and tissue repair to observe the cell viability and proliferation. On the other hand, MCF-7 is the human breast cancer line has been utilized. Therefore, ultrasound has been exposed to these cells to prevent cell proliferation and/or observe necrosis. In this way, ultrasound impacts have been evaluated in both ways regarding the cell viability and proliferation as a representative of in-stent restenosis treatment.

As a novel approach, to represent in-vivo conditions, PDMS substrates have been designed to replicate the vessel structure. Also, NiTi was selected as the representative biomaterial mostly used in vascular implants to culture the cell lines on it. After placing the NiTi surfaces into each well of PDMS substrates, cell lines have been seeded on NiTi. In this way, NiTi-based stents in direct contact with the target tissue have been simulated. Then, ultrasound energy is applied via ultrasound transducer which is directly coupled to the well. At this point, applying ultrasound to the NiTi surfaces located in the PDMS wells with cell culture on them has been another innovational attitude in this study. Cellular viability is evaluated after the sonication.

Regarding the medical use of ultrasound, it was claimed that the ultrasound application as a non-invasive treatment can be useful during and after the implantation

process to prevent any restenosis in a vessel and contribute to endothelization. For this purpose, ultrasound waves can be applied to the target tissue after implantation to prevent thrombosis, and because it is an easy-to-use method, patients with an implantable medical device such as vascular stents can apply ultrasound energy manually based on well-defined instructions themselves to achieve faster endothelization on the stent surfaces without hospitalization.

2. BACKGROUND AND THEORY

According to the World Health Organization's (WHO) findings in 20129, cardiovascular illnesses are the leading cause of death worldwide, accounting for 32 % of all deaths [2]. It is estimated that over 17.9 million people die each year as a result of these diseases over the world [2]. The number of patients who would die from cardiovascular diseases worldwide in 2030 is expected to be 23.6 million [1]. Turkey is experiencing a similar issue. Cardiovascular illnesses are the leading cause of death in Turkey, accounting for 47.7 % of all causes of death [32]. The leading causes of death from cardiovascular illnesses are coronary heart disease (7.3 million deaths) and stroke (6.2 million deaths). These premature deaths usually happen in patients under the age of 70 [2].

Atherosclerosis is the most prevalent and leading cause of coronary heart disease and stroke [6, 7, 13–15, 19], ischemic heart disease [7], hypertension [7], and peripheral vascular disease, etc.

The term "atherosclerosis" refers to a type of arteriosclerosis which is hardening, thickening, and structural change of the vessel [4, 33, 34]. There are three types of arteriosclerosis. Atherosclerosis, Mönckeberg's medial calcific sclerosis, and disease of tiny arteries/arterioles are the most common types [35]. In older people, vein hardening can cause abnormal changes in vein layers, changes in the elastic characteristics of the vein, and enlargement of the vein lumen, which is known as aneurysm disease.

Atherosclerosis is an inflammatory condition [14, 15, 36]. The mechanisms following the endothelial dysfunctionality which can be free radicals that may arise from smoking, hypertension, diabetes, and hereditary factors can contribute to the inflammatory process in the vein [7]. The permeability of the endothelium layer rises unless this defect is addressed by tissue remodeling. Lesions and atheromatous plaques form as a result of the accumulation of smooth muscle cells and collagen delivered to the

area [13]. Over time, atheromatous plaques increasingly collect in their structure as fat molecules, smooth muscle cells, collagens, elastin, etc [14]. Plaque evolvement produces a clog in the vessel, obstructing blood flow [14]. Angiography cannot identify occlusions until they occupy 45 % of the artery [37, 38]. Coronary restenosis, reoccurrence of stenosis, refers to a blockage that inhibits blood flow from the vein as the blockage grows in size and make narrower the vein [4]. A blockage in the coronary arteries can result in a heart attack [7, 13, 14] while a blockage in the cerebral vessels can result in a stroke [7, 12–14]. Fat layers and cell remnants that can separate from the plates over time can interact with blood coagulating substances on the endothelium surface, stimulating thrombus development [4]. Embolism from the thrombus may enter the bloodstream and induce venous blockage in another location [35].

Despite the fact that percutaneous coronary intervention (PCI) is currently the most often preferred technique for myocardial revascularization, coronary bypass surgery remains an essential part of the therapy of patients with severe obstructive coronary disease [39]. Bypass grafting - revascularization surgery - is commonly utilized as a therapeutic technique for atherosclerosis [16, 40]. Furthermore,PCI, an invasive technique, are conducted without surgery by inserting a guiding catheter through the skin into an artery [41]. These include stents, balloon angioplasty, lasers, and atherectomy [16]. During the angioplasty process, the balloon in the catheter is advanced through the skin from the arm or thigh bone to the target tissue [39]. By inflating the balloon, the plaque is pushed against the vessel wall, restoring blood flow [39]. A stent may also be inserted during this operation to maintain the artery open for a longer period of time. With recent advancements in expertise and technology, stenting has become the most widely applied method of PCI and may be preferable in numerous arterial occlusions and complicated lesions [36, 42].

Until 2017, the advancement of PCI and the significant milestones which can affect its widespread usage for clinical purpose is given in below Figure 2.1 [39]. These milestones contain progress in intracoronary imaging, supplementary antithrombotic and antiplatelet treatments, and hemodynamic lesion evaluation [39].

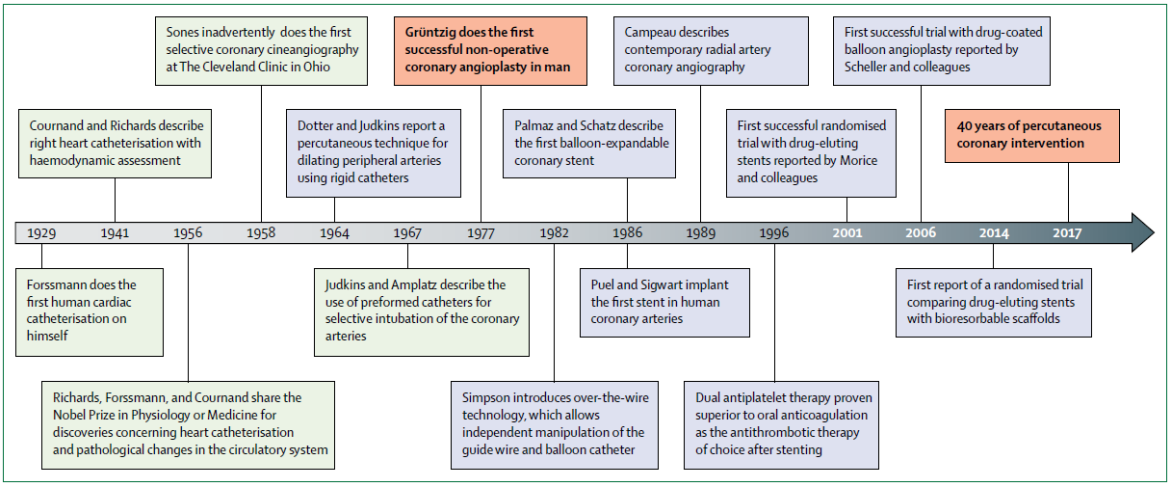

Figure 2.1 Advancement of Percutaneous Coronary Interventions until 2017 [39].

A vascular stent is a medical device with an expandable, artificial tubular structure that is used to restore obstructed blood flow in clogged blood arteries [43]. A catheter is used to advance the stent into the targeted anatomical location and it opens in the occlusion site and provides a pathway in the vessel for blood flow as shown in below Figure 2.2 [4].

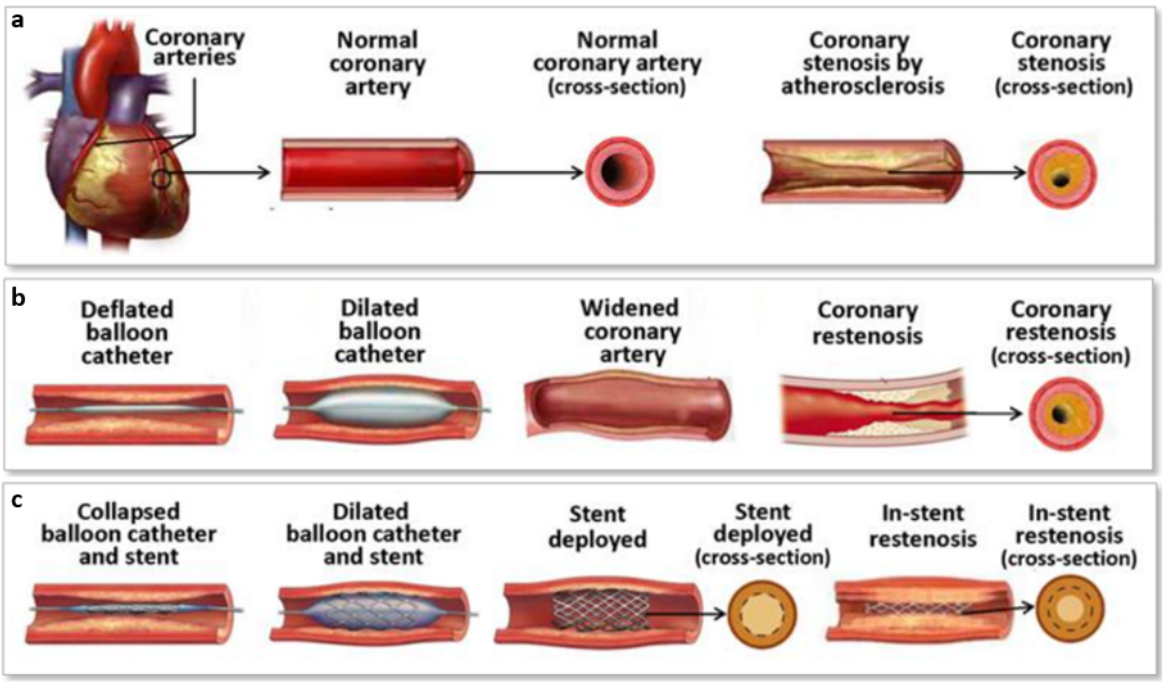

Figure 2.2 Representative picture of coronary stenosis by atherosclerosis (a), coronary restenosis (b), in-stent restenosis (c).

The formation of the coronary stenosis due to the atherosclerosis is shown in above Figure 1,a [4]. The coronary restenosis, was occurred after balloon catheter was dilated and widened the coronary artery, is demonstrated in Figure 1,b. Also, in-stent restenosis, which is the restenosis happened after the stent deployment was displayed in Figure 1,c.

Coronary stents range in diameter from 2.5 mm to 5.5 mm [44] and length from 8 to 38 mm [45]. The initial products of stent technology, which began in the 1980s, are bare metal stents (BMS) [5, 43, 46]. Today's metal stents are made of stainless steel (316L SS) [5, 39, 45, 47], titanium (Ti), platinum-chromium (Pt-Cr) [4, 39, 47], cobalt-chromium (Co-Cr) [4, 5, 39, 44, 47], cobalt-nickel (Co-Ni) [47] , nickel-titanium (Ni-Ti) [4, 5], platinum-cobalt (Pt-Co) [44] , platinum-iridium (Pt-Ir) [5], tantalum (Ta) [5], iron (Fe) [5], and magnesium (Mg) [5]. With the evolving stent technology, several vascular stent designs other than bare metal stents are now accessible. Stents with enhances surfaces, drug-coated, drug-eluting, polymer-integrated, bio-edible, self-opening stents are the most common examples [48].

Stents can also be categorized based on their manufacturing technique, geometric form, and substance [3, 49, 50]. Despite the fact that stent utilization is fairly widespread nowadays, it is necessary to understand and overcome some adverse effects and deficiencies [48]. In-stent restenosis (ISR) [48], stent thrombosis (ST) [48, 51], and infection [52] are the three most common ones. Thrombosis is classified as acute, sub-acute, late, or very late thrombosis based on the period of incidence [51]. Infection can lead to the development of thrombosis and restenosis [53]. The precise incidence of ISR is difficult to ascertain due to a variety of clinical, angiographic, and surgical conditions. Restenosis occurred among 32 to 55 % [5, 54] of all angioplasties prior to the use of stents, and dropped to 17–41 % in the BMS period [54]. Elastic contraction, inflammation, platelet deposition, neointimal formation, and arterial remodeling that differs based on the patient physiology are common processes that may induce to restenosis and thrombosis following PCI [55].

2.1 Classification of Stents

Based on the anatomical locations and clinical needs, there are different types of commercial vascular stents and their classification can be seen in Figure 2.3. In this thesis, instead of using tubular stent mesh structures, flat form stent metal (nitinol) has been used to evaluate endothelization on the stent surface and inhibition of smooth muscle cell growth which leads to obstruction in the vessel by applying ultrasound waves.

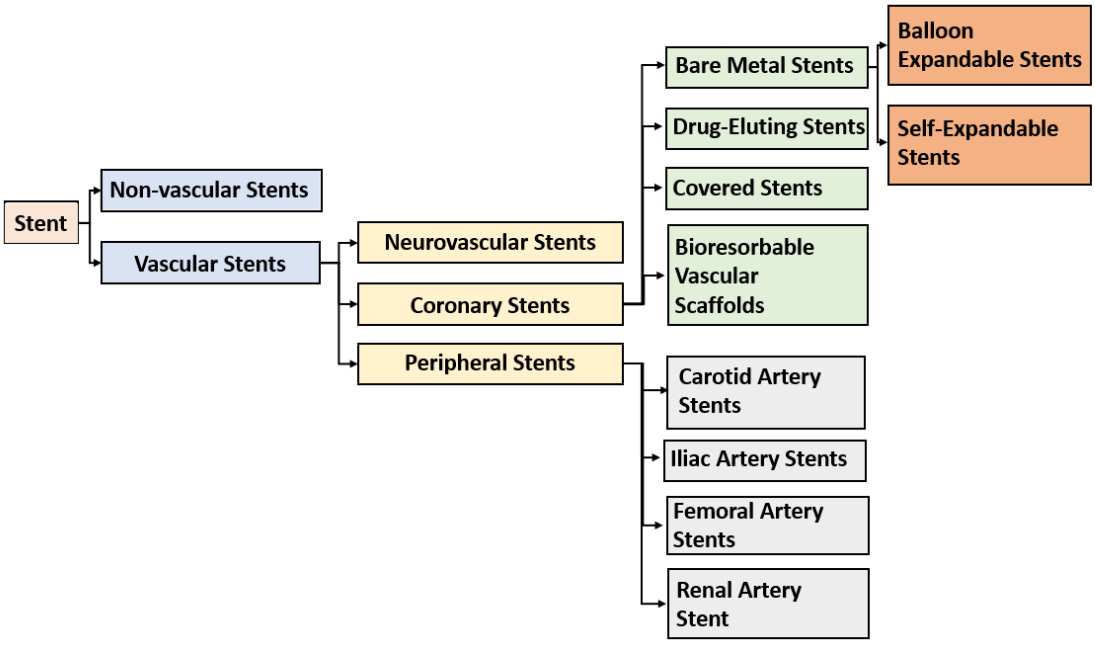

Figure 2.3 Classifications of stents [43],[46].

2.1.1 Coronary Stents

The coronary stent was invented in the 1980s [5, 43, 46] and has involved regarding the design, raw material, and structure [56]. There are mainly 4 types of coronary artery stents based on the material; Bare Metal Stent (BMS), Drug-Eluting Stent (DES), Covered Stent, and Bioresorbable Stent (BRS) [43].

2.1.1.1 Bare Metal Stents. The Bare Metal Stents (BMS) is a metal stent, composed of a metal such as stainless steel or cobalt chromium (Co-Cr), in the shape of a slotted tube or a coil [43] without coating or covering as sown in below Figure 2.4 [57]. This type of stent is utilized to achieve great strength as well as outstanding stretchability [43]. The primary idea behind BMS is to supply rigid mechanical support to the arterial walls while inhibiting artery recoil at the lesion location [48].

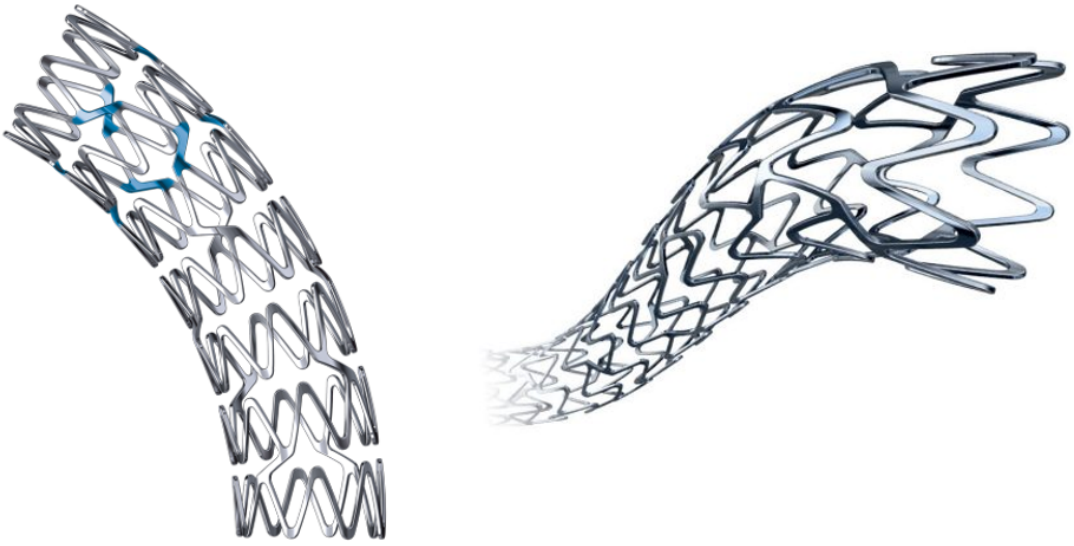

Figure 2.4 Boston Scientific, REBEL Stent System [57].

However, after the implantation of BMS, blood clots can develop rapidly due to the poor biocompatibility of metals within the human body, [43]. Endothelial dysfunction in the long term [4], inflammation [4] and thrombus development following the surgery [55] can lead to various adverse effects such as acute obstruction in the vessel and restenosis [43].

As an example, acute thrombus formation after BMS deployment as shown in below Figure 2.5.A [55]. Figure 2.5.B is the zoomed picture of A [55]. Also, attached cells to the elastic lamina can be observed in Figure 2.5.C after 3 days of the deployment [55]. In Figure 2.5.D, the neointimal hyperlapsia can be seen after 2 weeks of BMS deployment [55].

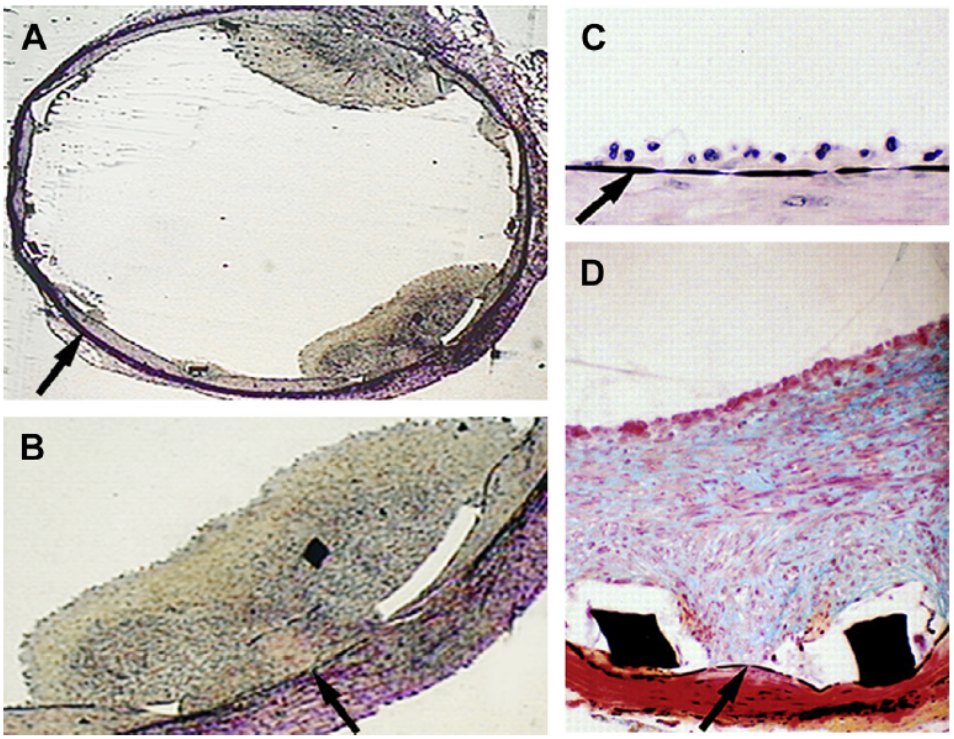

Figure 2.5 Thrombus formation after BMS deployment [56].

To avoid above side effects, DES has been evolved. The detailed evaluation of DES in Section 2.1.2. Also, there are two types of BMS; Balloon Expandable Stents (BES) and Self-Expandable Metal Stents (SEMS).

2.1.1.1.1. Balloon Expandable Stent

The Balloon Expandable Stent (BES) is a small, straight, solid medical device that are preserved by angioplasty balloon to prevent dislocation of the undeployed stent [58] by advancing with guiding catheters and compatible sheaths to be deployed into stenosis [47].

Below Figure 2.6 [47] depict the deployment of BES schematically. Firstly, BES is crimped onto the balloon catheter and advanced through the vessel to the target stenosed tissue. Then, the balloon is dilated and the stent is expanded, accordingly. It contributes to retain blood flow. Consequently, the catheter is removed, the balloon is collapsed, and the stent is deployed. In this way, the radial stiffness of a stent should

be assessed considering the expanded structure [47].

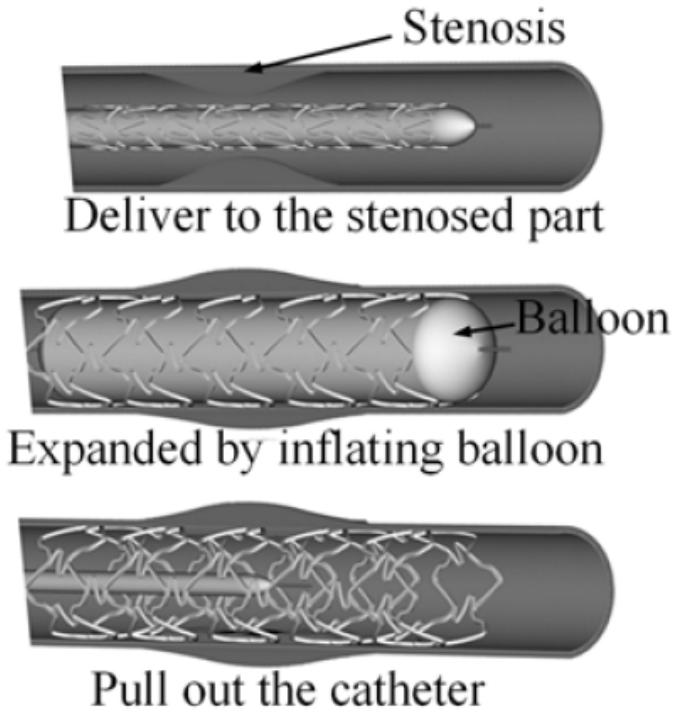

Figure 2.6 Schematic BES deployment process [47].

2.1.1.1.2.Self-Expandable Stent

Self-Expandable Stent (SEMS) are the flexible, expandable metal stents which can provide larger lumen [59], and wider patency [59] when the device is positioned and released from the delivery system in the target location [60]. Prior to release the device, fluoroscopic control can be made thanks to radiopaque marker as shown in below Figure 2.7.

Since there is no balloon needed during the implantation of SEMS, the size of the delivery system can be smaller compared to the BES delivery system [61]. Also, all SEMS can be buckled at lower pressures in comparison with BES. However, when the stress is removed, it can return back to its original shape [61].

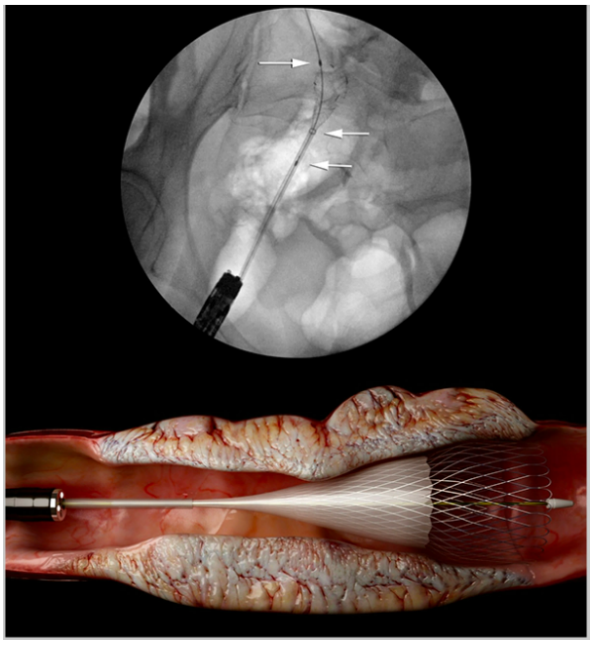

Figure 2.7 Wallflex SEMS placement and fluoroscopic control [59].

2.1.1.2 Drug-Eluting Stents. Stenting is a promising treatment for the atherosclerosis [10]. However, there is still high risks of restenosis after the stent deployment. It is significant to reduce the in-stent restenosis (ISR) since it can lead to stroke [10]. For this purpose, stent technology has been evolved to eliminate the estimated side effects such ISR and Drug-Eluting Stents (DES) have been invented [10, 21]. These stents release drugs which can inhibit the tissue growth lead to the obstruction in the stent, and aim to decrease the rate of restenosis in the coronary [4, 10, 21].

As demonstrated in below Figure 2.8, during the implantation procedure, the stent is firstly mounted to the balloon catheter and advanced into the vessel until reaching the tissue (Figure 2.8.A) [22]. Then, the stent is expanded by inflating the balloon (Figure 2.8.B) [22]. After the stent is implanted, the balloon is collapsed and removed (Figure 2.8.C) [22]. Therefore, the medication thanks to DES can be initiated in the vessel by releasing the drugs.

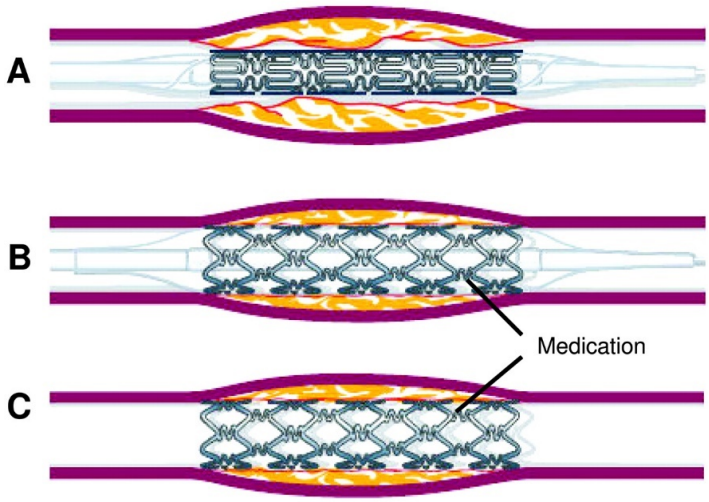

Figure 2.8 The representative image of the DES implantation [22].

DES structure is typically made up of a standard bare or coated metal stent as a platform, a polymer that regulates drug release by coating the drug, and a drug combined with the polymer [43]. Because DES differs from human tissue, there is still a chance of rejection when the stent is placed into the human body [43].

DES is regulated regarding the release rate of the drugs, which is based on the type and molecular weight of the polymer and the drug contained therein [43]. The materials used to cover the stent's surface should be blood and tissue compatible, non-toxic, and stable [43]. There are still some restrictions by using DES due to remaining the metal in a human body for a long time, possibility to re-operation, and/or generation of antiplatelet agents which increase the risk of bleeding [22, 43]. Although DES has some limitations especially after the deployment of the stent, it has a great potential for the treatment of CVD.

2.1.1.3 Covered Stents. Restenosis in the coronary vessels has made a remarkable progress. Although there have been good outcomes with evolving stent technology, there is still remaining risk regarding the restenosis [62]. At this point, the usage of covered stents is one of the innovative approaches that has a potential to eliminate the risk of restenosis [62].

Covered stents, which are metal stents covered by a polytetrafluoroethylene (PTFE) membrane [63] as the given example in below Figure 2.9 [64].

Figure 2.9 GETINGE, Advanta V12, Balloon expandable covered stent [63].

They can enable a direct barrier to ingrowth of neointimal hyperplasia and prevent to contact with the inflammatory tissue by sealing off [63]. In this way, they have been utilized to avoid restenosis, which is caused by tissue growth through the stent [63].

2.1.1.4 Bioresorbable Vascular Scaffold). Similar to DES, Bioresorbable Vascular Scaffold (BVS) can serve radial support to minimize vascular rebound by sealing intimal dissection after balloon angioplasty [65, 66]. Also, BVS can provide an opportunity to reduce the neointimal hyperplasia by antiproliferative drugs [65]. Fully degradation of BVS can be occurred after 3 to 4 years of the stent deployment and then it permits to re-endothelization and the recovery of the vessel [65]. Thus, the incidence rate of late scaffold thrombosis can be decreased [65]. Additionally, some of the problems related to the permanent metallic stents, such as late neoatherosclerosis, late stent thrombosis, and/or restenosis can be avoided [65, 66].

As shown in below Figure 2.10 [66], the three phases of BRS in terms of the functionality which are revascularization, restoration and reabsorption [66]. During the revascularization, the mechanical support can be preserved and the drug delivery process can be observed [66]. Secondly, the loss of the radial rigidity and mechanical restriction can be detected in the restoration phase [66]. Then, the resorption phase is occurred by losing the mass loss with vascular remodeling responses [66].

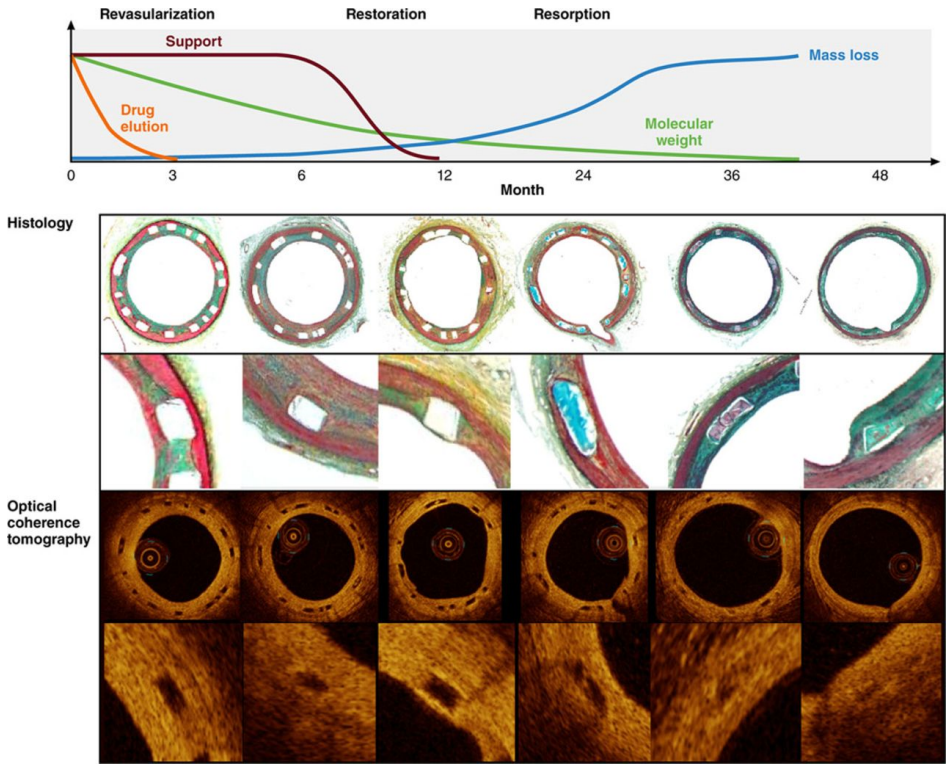

Figure 2.10 BRS functionality phases [66].

2.1.2 Peripheral Stents

Peripheral arterial disease (PAD) is a frequent and severe illness that mostly affects the lower limb arteries [67]. This disease affects around 3 to 10 % of the population aged 40–59, and 20 % of patients over the age of 70 [67].

In comparison with the open surgical revascularization, percutaneous transluminal angioplasty (PTA) has considerable advantages in terms of reduced patient morbidity [68]. Furthermore, PTA is linked to lower death rates in many of therapeutic scenarios. Thanks to the new technology and advancements in wire and catheter methods, greater success has been noted in several of these difficult locations [68].

2.1.2.1 Carotid Artery Stents. The carotid arteries run down either side of the neck, carrying blood and oxygen to the brain [69]. These arteries can become unhealthy with atherosclerosis over time, and plaque can generate on the interior, causing the vessels to make narrower [69]. This is called carotid artery stenosis. Smoking, high cholesterol, diabetes, age, and high blood pressure can be examples of risk factors for carotid artery stenosis [69]. As a solution, carotid artery stenting (CAS) has become the most preferred treatment method over the 30 years since it is the minimally invasive method with a low risk of cardiac injury [70]. The implantation procedure of the carotid artery stent is demonstrated in below Figure 2.11.

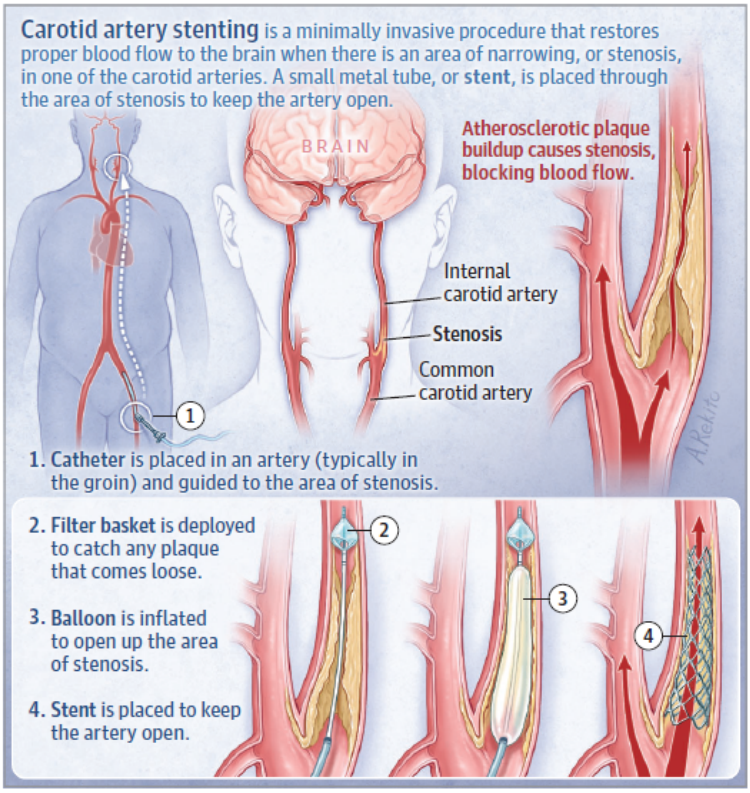

Figure 2.11 Representative image of carotid artery stenting procedure [67].

2.1.2.2 Iliac Artery Stents. PTA is becoming increasingly significant in the treatment of ischemia caused by iliac artery occlusive disease [68]. PTA is currently considered the major therapeutic option for stenotic lesions that do not have full occlusion and include relatively small portions of the artery (5-10 cm) [68]. Furthermore, PTA can effectively treat localized total occlusions of the common iliac artery with long-term patency rates comparable to open surgical revascularization [68].In the treatment of patients with critical limb ischemia and several degrees of arterial blockage, iliac artery angioplasty has been utilized successfully with infrainguinal surgical revascularization [68]. The iliac occlusive disease PTA offers optimum vascular inflow to the femoral artery level [68].

Many of patients with aortoiliac PAD have disease patterns that are suitable for endovascular treatments, such as stenting, which accomplished in high success rates and good durability [71]. Open surgical treatment is still a highly effective option for patients with severe occlusions such as bilateral iliac arteries or those who have failed

before endovascular interventions [71].

As an example, the stent implantation procedure into the left common iliac artery can be shown in below Figure 2.12. There is a high-grade of stenosis above the bifurcation as indicated with red arrow in Figure 2.12.a, and the large lumbar collaterals can be seen above the stenosis remarked with white arrow [71]. In Figure 2.12.b, stents located into both aorta and bilateral iliac arteries can be seen by fluoroscopic image [71]. Aortic restenosis is marked with red arrow in Figure 2.12.b [71]. In this patient, completion angiography reveals broadly patent aortoiliac artery stents with clearance of the stenosis in Figure 2.12.c [71]. Angiogram of separate patients demonstrates the total blockage of the left common iliac artery to the aortic bifurcation by red arrow in Figure 2.12.d [71]. Flow restoration in here shows the blocked segment's end (red arrow in Figure 2.12.e) [71]. Also, by insertion of stents (red arrows), the occluded artery was successfully reopened shown in Figure 2.12.f [71].

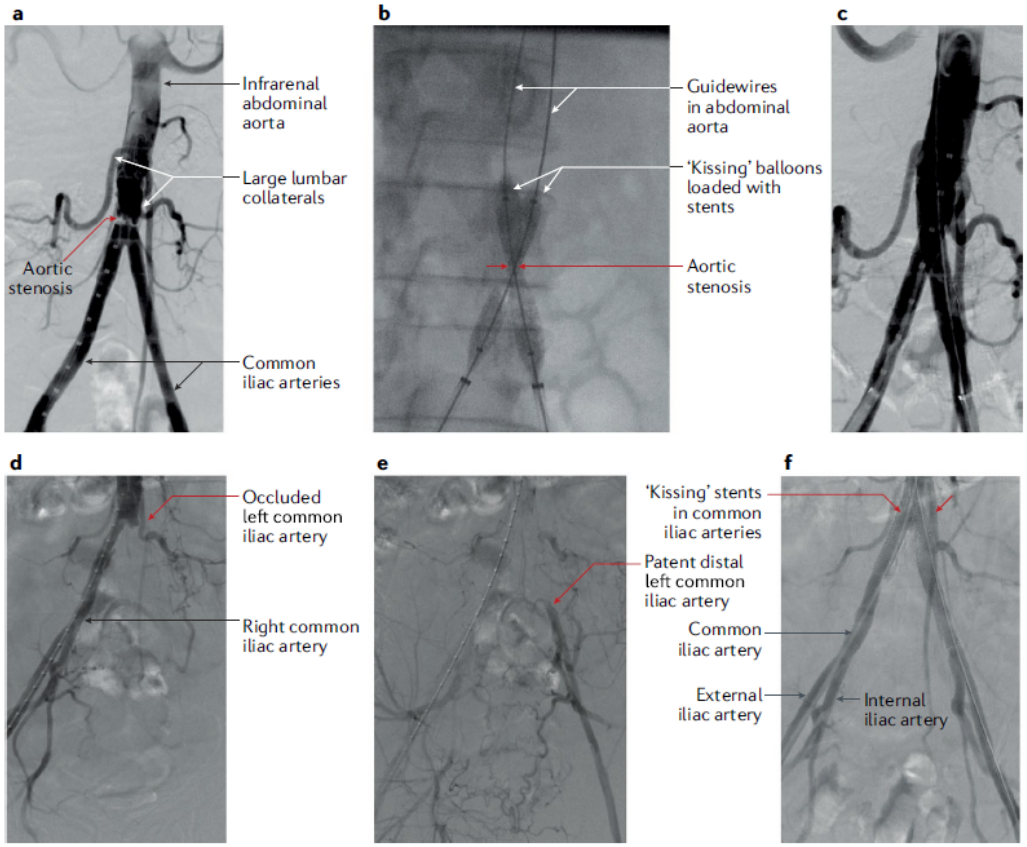

Figure 2.12 Aortoiliac intervention for PAD [71].

2.1.2.3 Femoral Artery Stents. Femoral artery stenting is the minimally invasive procedure to open obstructed femoral artery by a stent deployment. One of the most well-known vascular disorders is stenosis of the femoral artery [72]. Similar to the carotid or coronary artery diseases, the plaque formation can be occurred in the leg vein. Therefore, the narrowed blood vessel of the patients can be opened by minimally invasive operation such as balloon angioplasty or stent deployment [73]. In addition to that, PTA has been utilized for the treatment of the occlusion in the femoral artery by stent deployment [72].

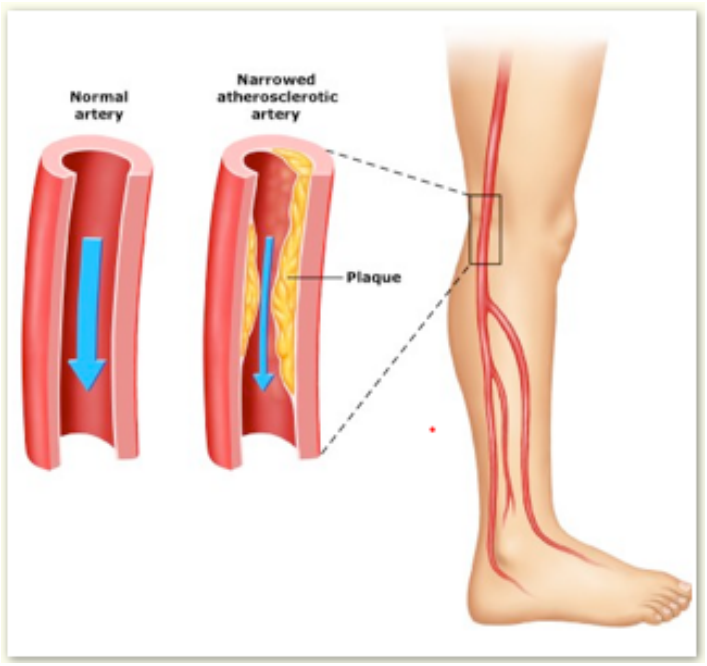

Figure 2.13 Representative image of plaque formation in the femoral artery [73].

2.1.2.4 Renal Artery Stents. Renal arteries are in charge of the blood transportation to the kidney. When they have been obstructed or became narrower due to the atherosclerosis which is mostly related with the hypertension [74, 75], renal artery stenting procedure can be used to reopen the blood vessel and retain the blood flow by angioplasty [76] as shown in below Figure 2.14 [77].

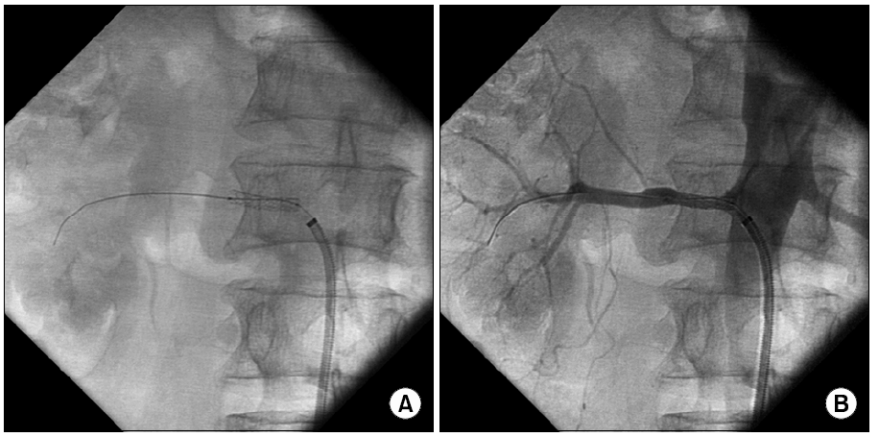

Figure 2.14 Renal Artery Stent Implantation [77].

2.2 Ultrasound Therapy

Therapeutic ultrasound (TUS) is a promising method to stimulate cells by increasing biological activity such as endothelization [78–80] among several new medical applications for local treatment [81]. For instance, ultrasonography for the carotid artery is a long-standing and dependable technique for diagnostic modalities used to detect vascular morbidity in a preliminary stage [82]. Furthermore, since the carotid arteries, are in charge of transportation of the blood to the braid, are placed into each side of the neck, ultrasound waves can easily be applied to detect the obstructed or narrowed carotid arteries [83] as shown in below Figure 2.15 [84].

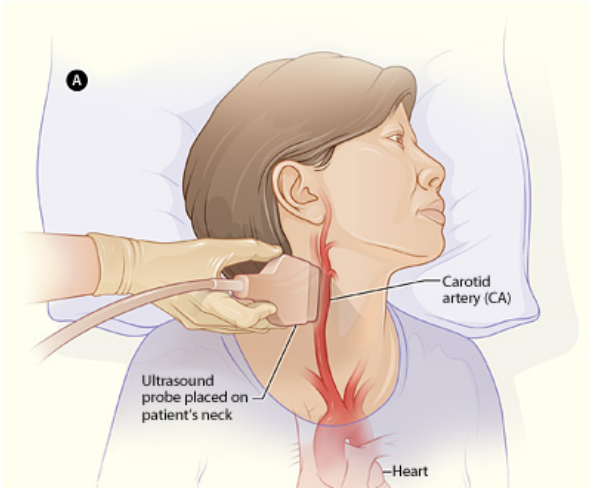

Figure 2.15 Representative image of ultrasound application to the carotid artery [84].

In addition to the invasive treatments, many experiments showed that the ultrasound can prevent tissue occlusion such as atherosclerotic plaques [85]. According to the findings by Zhang et. al., there were no patients who withdrew from the ultrasound therapy due to adverse effects. After the treatment, the maximum thickness and area of 79.94 % of the carotid plaques in the ultrasonic group were decreased, whereas the thickness and area of 18.52 % of the plaques in the control group were reduced [85].

Considering that, further experiments will be performed with carotid artery cell to define the ultrasound wave impacts on them. However, in this thesis, as a preliminary study of the evaluation of ultrasound application, it has been performed to see cell viability and proliferation of fibroblasts as a representative of endothelization, and cell damage of MCF-7 cells to simulate providing the plaque formation in the vessel.

Since ultrasound therapy has been applied in many clinical applications [86,87], and in-vivo studies [88] owing to its contribution to endothelization, wound healing process, and enhancement in tissue repair, fibroblast cells have been widely studied in TUS applications [79, 89–92]. However, the underlying mechanisms of ultrasound in wound healing and tissue repair are not entirely understood [80, 90].

In-vitro studies have shown that ultrasound may directly or indirectly affect the potential mechanisms involved in blood flow, inflammation, cell migration and cell viability, angiogenesis [93], gene expression, etc. [94]. It triggers cellular pathways [95, 96] leading to the proliferation of cells such as fibroblast [79, 81], osteoblasts [97], monocytes [97], endothelial cells [98]. On the other hand, ultrasound may also have potential risk factors to cellular mechanisms and patient safety through formations of free radicals and/or deoxyribonucleic acid (DNA) damage [99–101]. Although high-intensity ultrasound tends to exhibit damaging effects, the threshold of the safety level has not been observed for high-intensity nor low-intensity ultrasound. Furthermore, a consensus has not been achieved for the ultrasound dosages for proper application of any cell type. The reason is the variety of the applied dosages, cell type, studied assay, and the experimental set-up [97].

One of the application areas of TUS is breast cancer necrosis with different dosages [101–104]. Since breast cancer is one of the most frequent types of cancer in women, it is crucial to inhibit cell growth and/or keep it under control [102]. MCF-7 human breast cancer cell line has been one of the most preferred cell lines for many years to contribute to cancer research globally, and it can provide the practical knowledge to accelerate the treatment process considering patient care [105].

As a routine treatment method, ultrasound therapy for human breast cancer cells can be implemented [106,107] because the complication rate after the treatment is very low [106]. Therefore, it is beneficial for localized breast cancer since the ultrasound can enter the tissues with the low energy fading [107]. Also, no severe adverse events have been observed in adjacent tissues after the application [108].

2.3 Nitinol

Nitinol (NiTi), a nickel and titanium alloy, is a widely used biomaterial due to its unique material specifications such as high biocompatibility, super elasticity, shape memory performance, and excellent mechanical performance [28, 29, 109, 110].

Super elasticity refers to the property of an alloy to turn back to the original shape by a constant force and a large, reversible, and substantial deformation [29, 111, 112]. It occurs when the test temperature is above the austenite finish (Af) temperature or in between austenite start (As) and Af temperatures. As seen in Figure 2.16, when stress is applied to the material in the austenite phase, it transitions to a stress induced martensite phase (Figure 2.16.b). When the stress is removed, the material can transition back to the austenite phase and thus its original shape again (Figure 2.16.c) [28].

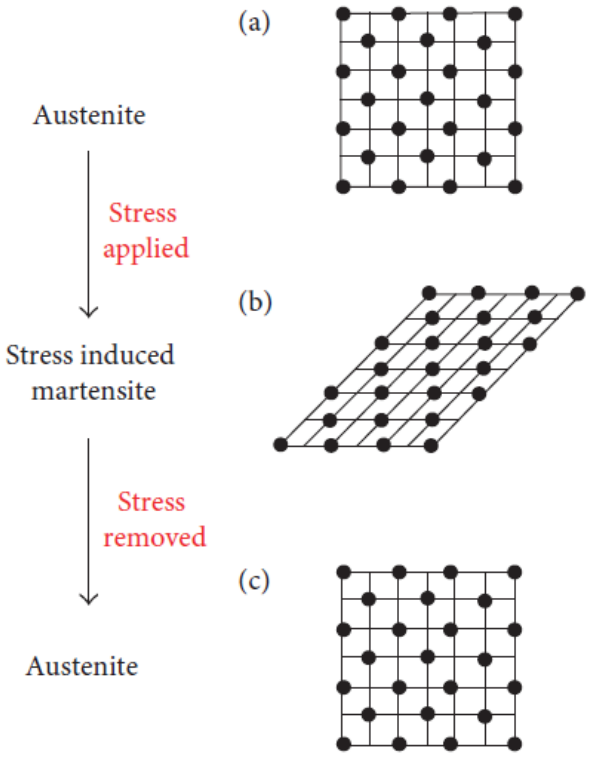

Figure 2.16 Super elasticity property of NiTi [28].

Moreover, NiTi, as a shape-memory alloy (SMA), has the ability to recover to its original shape. Different from the super elasticity, the material is mostly in the martensite phase for the shape memory performance. When stress is applied, the material is in a detwinned martensite form. When the stress is removed, the material can maintain its detwinned martensite form. When the detwinned martensite form of the material is exposed to heat, it transitions to the austenite phase. After cooling the material, the material's shape defined [28].

A significant material property of NiTi alloys is its biocompatibility. NiTi alloys have been well-tolerated by the patients due to good corrosion resistance in the human body [28, 30, 111]. Moreover, it was proven that NiTi has no toxic effects and accordingly, cell viability and proliferation are usually observed during direct contact of tissue with NiTi [29, 30].

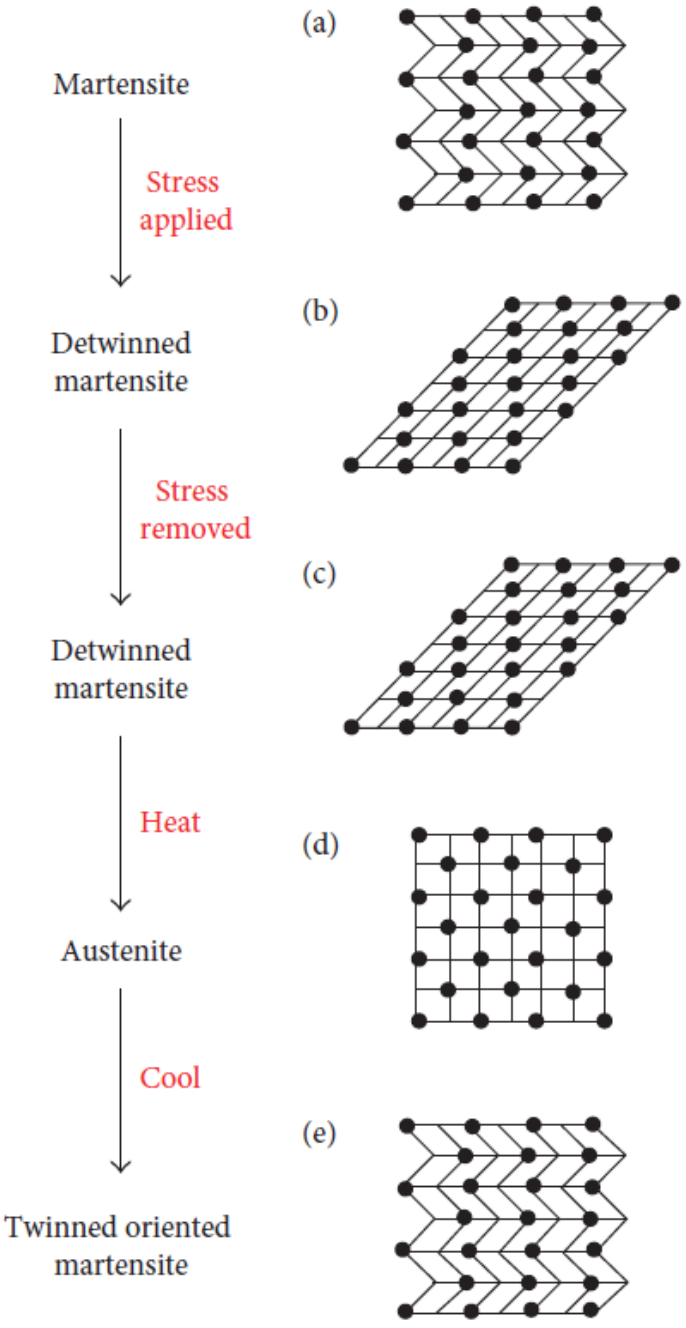

Figure 2.17 Shape memory property of NiTi [28].

NiTi is a self-passivating biomaterial which can form a stable surface oxide layer to prevent any corrosive effect to the material [112, 113]. On the other hand, since the NiTi alloys contain high amount of nickel, it may cause allergic reactions, or disorders which may prevent proliferatation of healthy cells [29]. Additionally, the exposure of the high levels of nickel to the blood circulation can be hazardous for the patient care owing to excessive corrosion and may lead to some adverse events [113]. At this point, the effects of nickel and titanium have been compared and the results show that while the nickel can cause harmful effects on cellular activity, the nitinol alloy which comprises of nickel and titanium reacts the same as titanium, totally inert [29]. Moreover, the same study has evaluated the effects of nitinol, stainles steel, and titanium on the osteoblasts and the fibroblasts. The results proved that there is no toxic impact of nitinol on these cells [29]. Furthermore, many researches have shown that in long-term follow-ups, nickel levels in the blood have not significantly increased and caused any toxicity [29, 112–115].

In light of all these unique material specifications, NiTi alloys are usually preferred for medical purposes. For instance, thanks to the elasticity of NiTi, NiTi needles have been manufactured and utilized for surgical operations [30]. The thermal shape memory properties of NiTi have allowed for the development of the closure device contributing to bone healing [30]. Another device made by NiTi is the vena cava filter, which is implanted into the vena cava by advancing the device through a compatible delivery system to place the device in the target tissue and prevent any thrombus formation [30].

One of the main application areas of NiTi alloys is in stent technologies [28, 29]. The first products of stent technology, which started in the 1980s, are bare metal stents [46]. In the top figure, the stent were compressed for the transcatheter replacement, while in the bottom one, it can return back to the original shape after heat exposure.

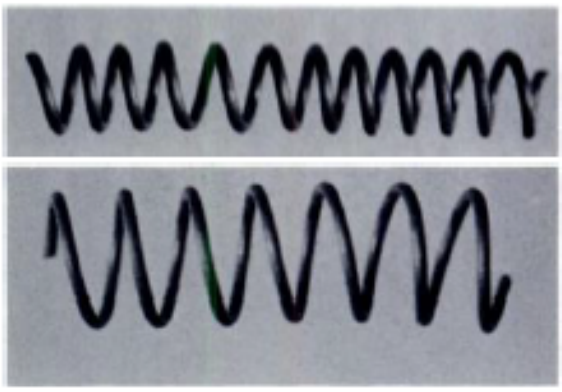

Figure 2.18 First bare metal stent [47].

Another utilization of NiTi is for the tracheobronchial stent to investigate axial buckling [116]. The device design can be seen below in Figure 2.19. Due to the superelastic properties of NiTi, it was claimed that the the tracheobronchial stents made by NiTi can be a good approach for self expandable stents.

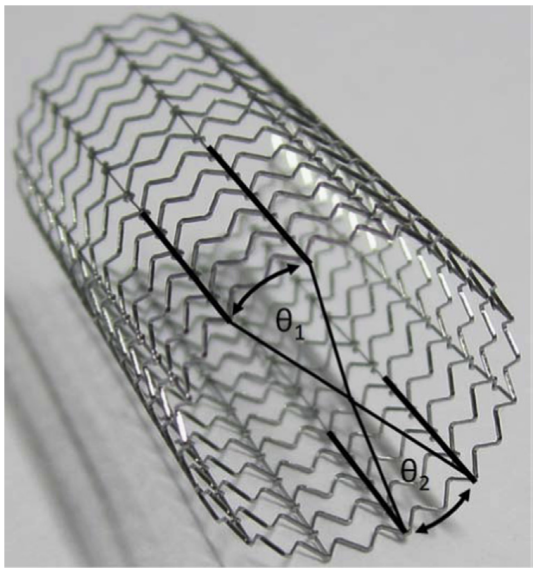

Figure 2.19 Stent for axial buckling [116].

In a other study, NiTi alloys have been preferred to manufacture coronary artery stents owing to its radiopacity, super elasticity, and the shape memory performance. As a result of in-vitro cytotoxicity studies and in-vivo biocompatibility studies, the fabricated coronary stent, shown below in Figure 2.20, has been found as highly biocompatible. Also, according to the cell proliferation test, it was proven that these NiTi

coronary stents have good cytocompatibility [117].

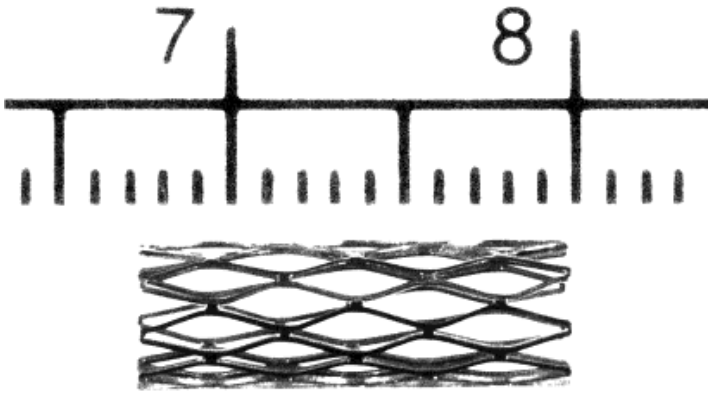

Figure 2.20 Coronary stent example [117].

In addition to all, NiTi-based stents have been commonly utilized for the carotid artery stents due to its unique properties such as being self-expandable [118, 119] and shape memory alloy [118, 119], super-elasticity [119], biocompatibility [118, 119], and excellent corrosion resistance [119]. Many of the researches have been evaluate the safety of the braided, expandable, NiTi stents for the carotid artery stenosis regarding the in-stent restenosis and thrombus formation [119, 120].

Ahlhelm et. al. [120] have been implanted NiTi based laser cut stent (shown in below Figure 2.21) to the porcine model and they have been accomplished to stent deployment without any complication. Although the NiTi stents have been observed to generate a thicker neointima before, no thrombosis or greater than > 60 in-stent-stenosis was detected in this study [120].

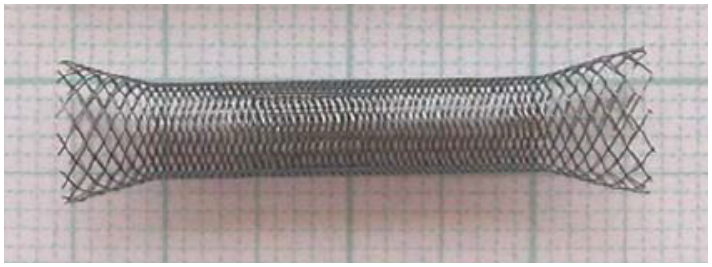

Figure 2.21 Testing NiTi stent [120].

As an example of Ni-Ti based carotid artery stents, The Roadsaver stent (Terumo Interventional Systems) [121] can be evaluated [18]. It is designed for the carotid arterial atherosclerotic. The Roadsaver stent is composed of double layer NiTi mesh design as shown in below Figure 2.22 [18] to eliminate the plaque formation and embolization after the stent deployment [121]. Since there are many micromesh cells into the stent, it can behave like a covered stent [18]. Also, due to the NiTi, it provides good flexibility, wall apposition, and permits patency for the side branch [121].

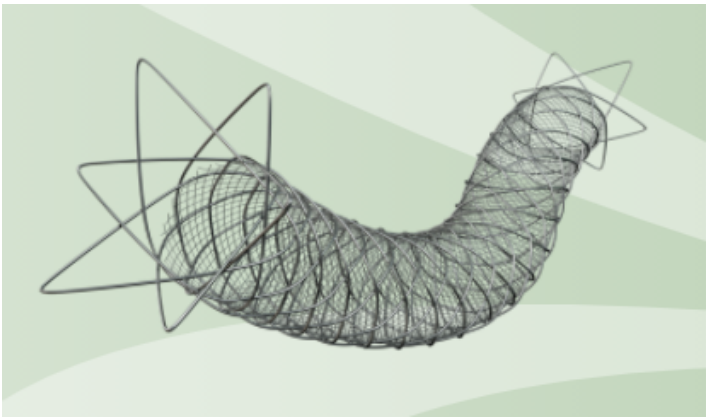

Figure 2.22 Roadsaver Carotid Artery Stent , TERUMO Interventional Systems [121].

Another NiTi-based carotid stent example is The Gore Carotid Stent (W. L. Gore & Associates) [18]. According to Schönholz et. al., the simple handling and safety procedure of 6 mm,8 mm, 40 mm Gore Carotid Stent can be achieved and based on the findings at the end of 6 month after the surgery, they detected stent patency, preservation against the emboli generation, and compatibleness to the tissue wall [18].

In light of these examples, it can be concluded that NiTi based stents can be useful for the carotid artery occlusion. Since the further studies will be focused on the carotid artery diseases, this preliminary studies with NiTi can be a promising approach.

In conclusion, NiTi alloys have been extensively used in stents for a wide variety of medical purposes. It is now expected to generate a US 16.666 billion dollar industry by 2022 [122]. Half of these stents are being foreseen to be made of nitinol [29].

In this thesis, NiTi surfaces have been utilized as a representation of stent technology. The cell lines used have been cultured on these NiTi surfaces. Then, the ultrasound application has been performed at different dosages to these cell lines in order to evaluate the sonication effect regarding the cellular viability and endothelization on the stent accordingly.

2.4 Polydimethylsiloxane (PDMS)

PDMS is a polymer which is one of the silicone elastomers [23, 25]. Since it can provide many advantages, PDMS has a wide variety of application areas such as biomedical, mechanical, or electronic industries [23].

In the biomedical device industry, PDMS is a well-known biomaterial due to its biocompatibility, non-cytotoxicity, ease to manufacture and use, optical transparency, elasticity, permeability, similarities to some biological tissues, ability to mimic some circular vascularized structures, chemically and thermally stability, low cost, and time-saving properties [23–26].

In recent years, many research gropus are attempting to mimic micro environment of the human body by designing in-vitro experimental setups to get fast and cost-effective responses [23, 26]. For this purpose, PDMS is an extensively preferred biomaterial, especially for tissue mimicking, simulating the vessel structure, and/or multilayer vascular model phantom owing to its ability to imitate the complex structures such as circular blood vessel in micro dimension [23–26].

Taking into account these material specifications of PDMS, it is inevitable to use it for medical purposes. For instance, PDMS has been utilized to prevent aneurysm in the blood vessel by understanding the biological and mechanical responses [123], replicate the circular blood vessel structure in the micro-cardiovascular system and enable endothelial cell growth on it [26], and to fabricate transparent and flexible tubing to simulate multilayered structure of five peripheral tissues which are epidermis,

hypodermis, blood vessels, and blood [24].

All things considered, PDMS has been selected to constitute the vessel structure in this thesis. The basic similarities among PDMS and vessel structures can be found in below Table 2.1.

Table 2.1
Comparison of PDMS and Vessel Structure

Properties	**PDMS**	**Vessel Structure**
Thickness	$1.1mm$	$1.14 \pm 0.10mmforvein$
Elasticity	✓	✓
Permeability	✓	✓
Flexibility	✓	✓
Multilayer Structure	✓	✓
Compressibility in particular momentum	✓	✓

In this way, the human body response after the stent implantation regarding the endothelization can be evaluated by an in-vitro setup.

2.5 Cell Culture Studies

As a preliminary study for the evaluation of ultrasound exposure effects, two different cell lines were used. One of them is L929 fibroblast cells (American Type of Culture Collection (ATCC), CCL 1), which plan an important role for some physiological activities such as producing extracellular matrix (ECM), wound healing, and bone repair. Therefore, it was aimed to retain the cell viability and proliferation of fibroblasts.

Furthermore, since MCF-7 human breast cancer is very common disease especially for women, it is very essential to prevent cell growth and enable necrosis by some

therapeutic approaches such as ultrasound. For this purpose, MCF-7 human breast cancer cells (ATCC, CRL 3435) were chosen to study the various effects of ultrasound waves.

The main goal for choosing these cell lines is to evaluate different ultrasound impacts on different cell lines such as fibroblast cells and MCF-7 cancer cells. While it is very crucial to see cell proliferation of fibroblasts following ultrasound exposure, ultrasound waves are applied to MCF-7 cell lines to prevent cell proliferation and/or observe cell damage. In this way, it can be claimed that ultrasound can be a useful method for both cell proliferation such as endothelization and cell damage like the prohibition of any occlusion in the artery that causes atherosclerosis.

2.5.1 Alamar Blue (AB) Cell Viability Assay

Briefly, AB is one of the non-toxic cell viability reagents. It contains resazurin, a fluorescent blue indicator dye. It is generally used as an oxidation-reduction (REDOX) indicator and it can provide the colorimetric change for the cellular, and metabolic reduction [124, 125]. The reduced form of resazurin is called as resorufin, is highly fluorescent [124, 125].Therefore, the intensity of the fluorescence produced is directly proportional to the number of living cells [124, 125]. Thus, AB can be utilized as an indicator for the healthy cells.

2.5.2 Acridine Orange (AO) and Propidium Iodide (PI) Staining for Cell Viability

As a simple, and rapid application, Acridine orange (AO) and propidium iodide (PI) are mostly preferred nucleic acid-binding dyes to prove cell viability [126]. They are utlized as a fluorescent marker to visiualize cellular viability simultaneousl [126].AO can enter the living cells as an inclusion dye and lead to cell to propagate green fluorescence while PI as an exclusion dye cannot go into the living cells but can penetrate into the

dead cells to fluoresce red by binding the nucleic acids [126]. In this way, live and dead cells after the staining can be distinguishable easily.

2.5.3 Immunofluorescence staining with 4', 6-diamidino-2-phenylindole (DAPI) and F-actin

Immunofluorescence is a light microscopy method utilizing a fluorescence microscope that is mostly utilized on microbiological samples. This approach employs the specificity of antibodies to their antigen to direct fluorescent dyes to specific biomolecule targets within a cell, allowing observation of the target molecule's distribution throughout the sample [127].

Immunofluorescence can be used to examine the distribution of proteins, glycans, and tiny biological and non-biological substances in tissue slices, cultured cell lines, or individual cells. This method can even be utilized to observe the things like intermediate-sized filaments. If the topology of a cell membrane has not yet been defined, immunofluorescence and epitope insertion into proteins can be employed to identify structures. Also, it can be used in conjunction with other non-antibody fluorescent staining techniques, such as the use of DAPI to mark DNA [127].

Actin is a family of globular multi-functional proteins that form microfilaments and can be a free monomer called G-actin or part of a linear polymer microfilament called F-actin [128]. Actin stains are utilized to detect the live and fixed cells to define their structure, cytoskeleton functionality [129]. In this thesis, Phalloidin- iFluor 488 Reagent (abcam, UK) was used. It can be bound with actin filaments and then the living cells can generate green fluorescence while investigating them under the fluorescent microscope. Additionally, DAPI was practiced to visualize the nuclear DNA in both live and fixed cells [130]. It is a blue fluorescent DNA stain and excited by the violet laser line [131]. Therefore, the cells which are exposed to DAPI as nuclear counterstrain can be observed under the fluorescent microscope.

3. MATERIALS AND METHODS

During the experiments, each step shown in below flow chart were examined, respectively.

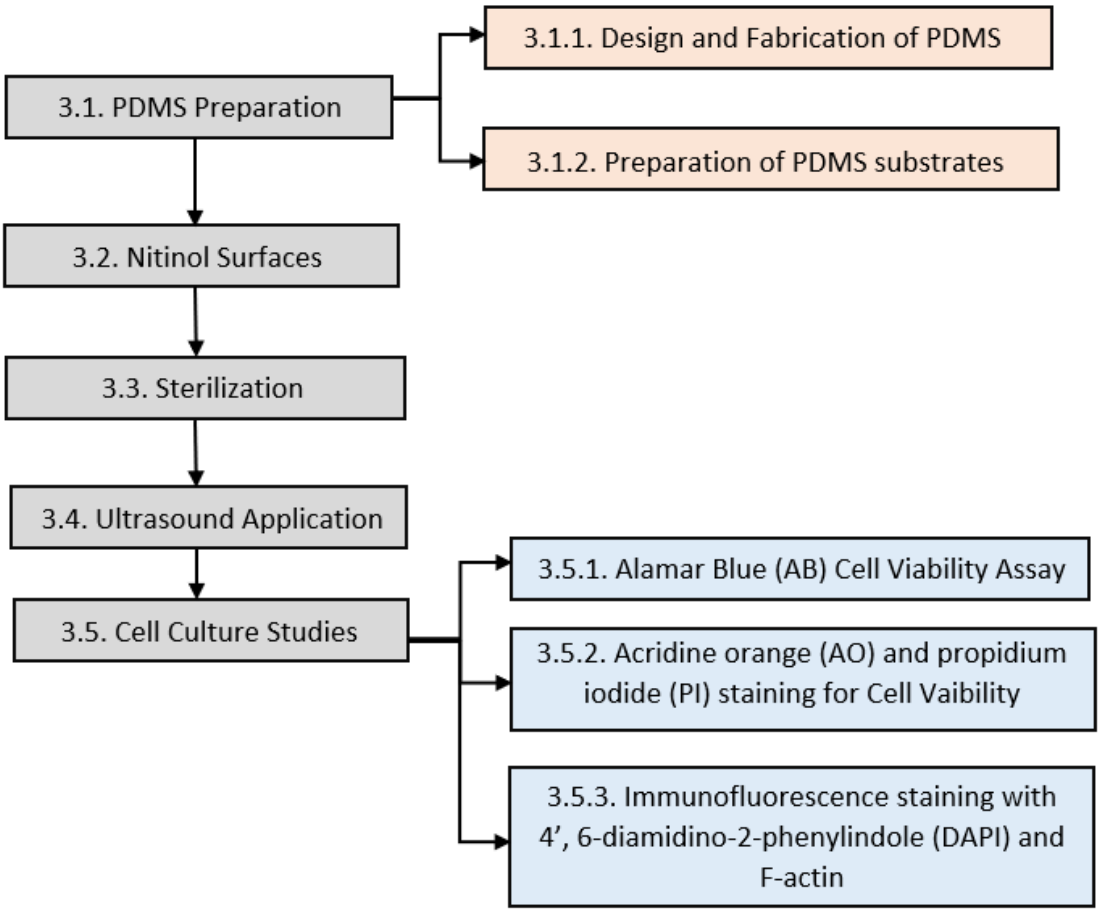

Figure 3.1 Flow Chart of the Experiments.

3.1 PDMS Preparation

Preparation of PDMS substrates includes two main steps; design and fabrication of the molds which PDMS is poured into, and preparation of the PDMS.

3.1.1 Design and Fabrication of PDMS Molds

The customized PDMS molds, PDMS substrates have been poured into them, have been designed by using Computer Aided Design (CAD) software (Siemens Solid Edge). For the design process, CAD programs are user-friendly methods because the required modifications can be performed easily considering the needs of the application.

For this study, PDMS molds have been designed as shown in below Figure 3.2. Each dimension can be found in this Figure as well. There are four circular parts in each mold to create wells as a representation of the vessel structure.

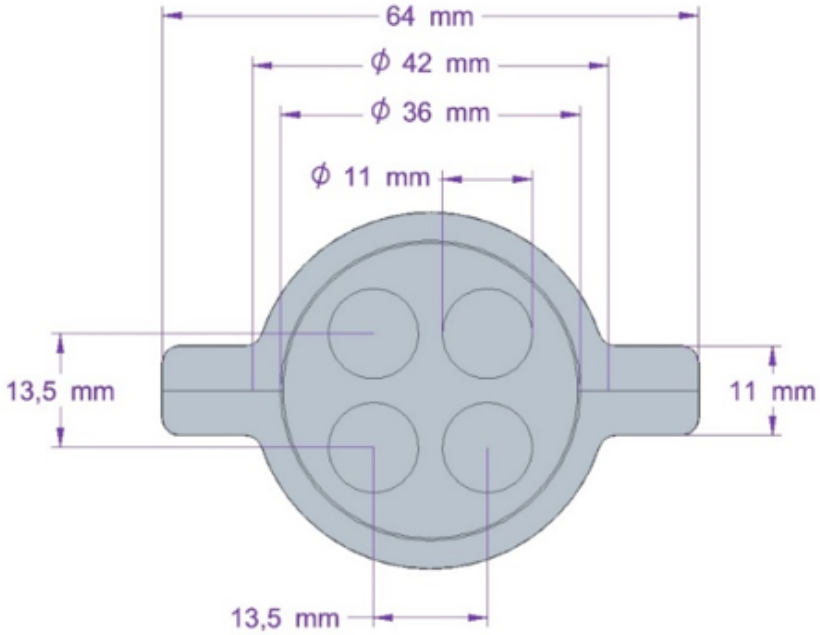

Figure 3.2 Technical Drawing of PDMS Molds.

Since the ultrasound waves have been applied to the bottom of the PDMS substrate, the thickness of the base part was determined as 11 mm considering the thicknesses of human and phantom skin, vessel wall and blood [24] as shown in below Figure 3.3.

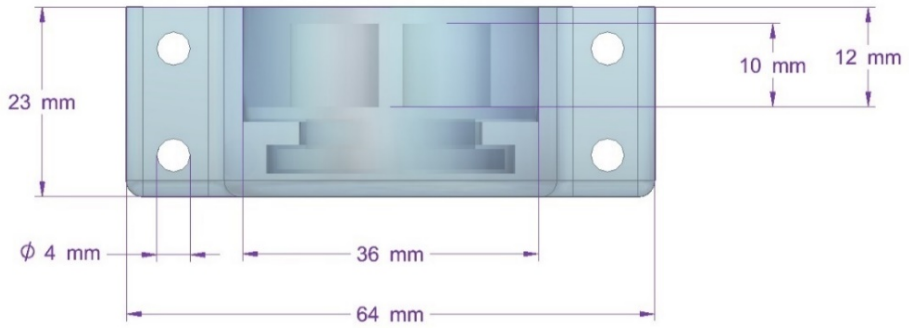

Figure 3.3 Technical Drawing of PDMS Molds.

Each mold consists of three separate parts and the main structure is constituted by assembling these three parts as it can be shown in below Figure 3.4.

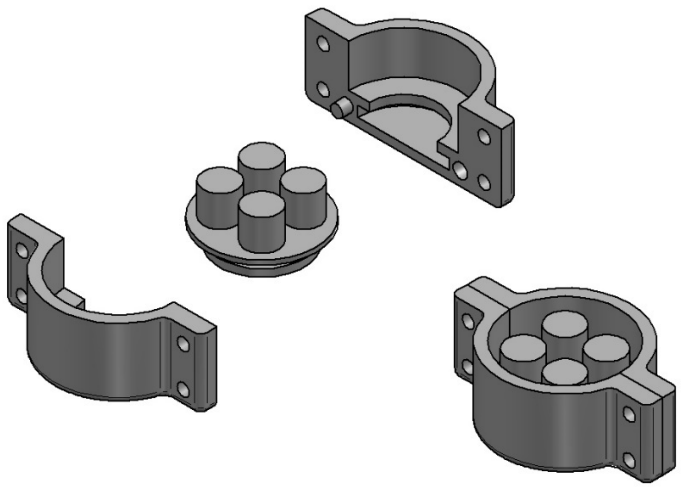

Figure 3.4 Representative pictures of PDMS Molds.

The dimensions of each part can be found in below Figure 3.5.

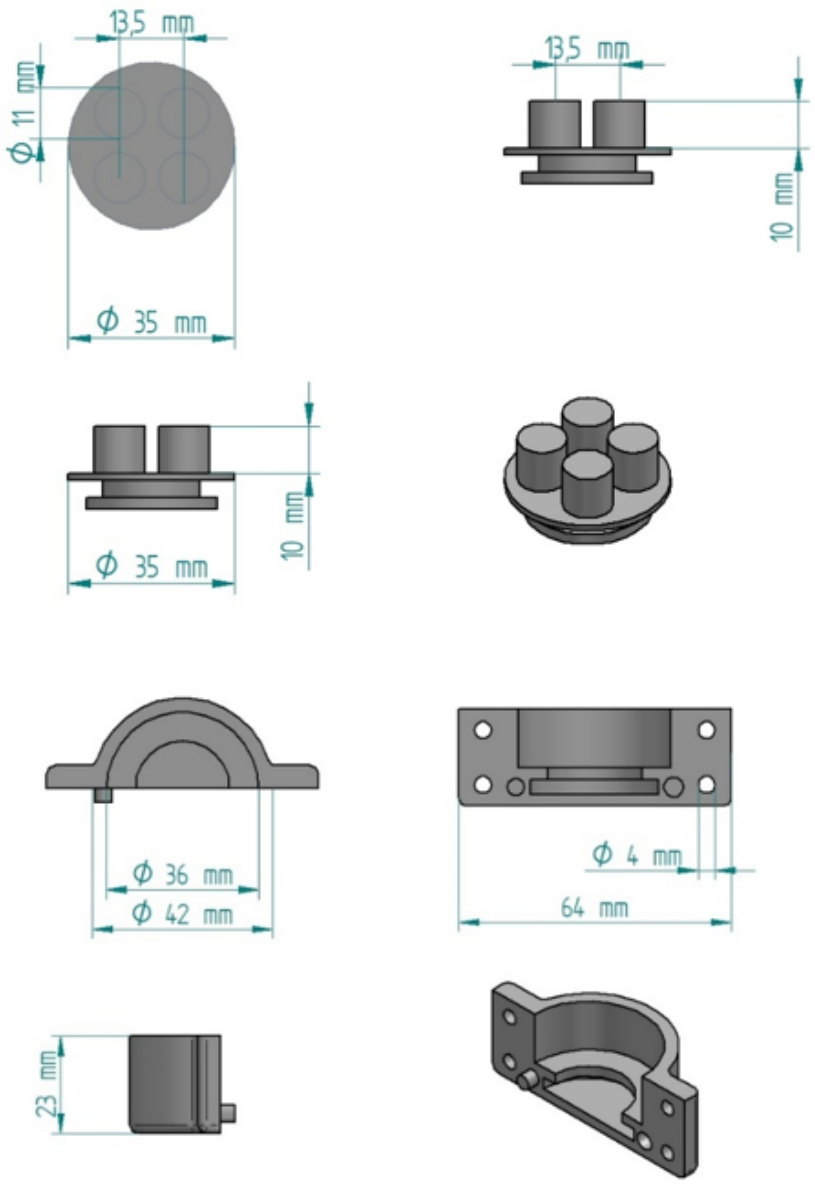

Figure 3.5 Dimensions of each part.

After the technical drawings have been completed, the CAD file has been converted to three dimensional (3D) printing file with .stl extension by the slice program Z-Suite. It has been prepared with the high resolution to get smoother surfaces. Then, each part has been printed by Zortrax M200 Plus printer with polylactide (PLA) as a printing material.

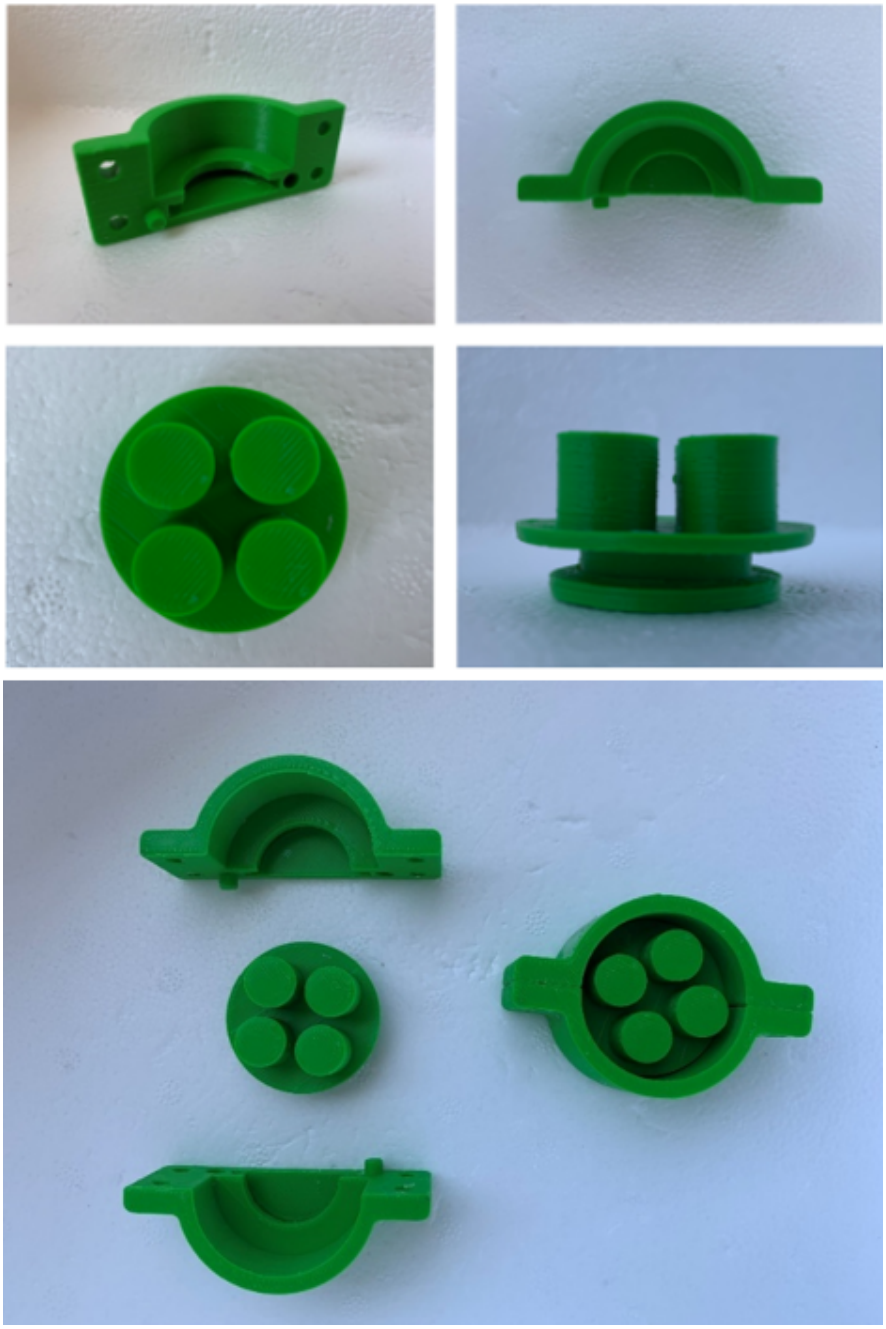

Figure 3.6 Parts of PDMS molds.

3.1.2 Preparation of PDMS Molds

PDMS substrates have been prepared by mixing SYLGARD 184 Silicone Elastomer Base and SYLGARD 184 Silicone Elastomer Curing Agent. The ratio of the silicone elastomer base and the curing agent is 10:1 by weight. For this purpose, the accurate measurement has been performed by the precision scale (Sartorius GL224i-1CEU). Afterwards, PDMS has been mixed and then degassed by the desiccator (Rocker 300) to prevent bubble holes formation during curing. Next, PDMS was poured into the 3d-printed molds and it was put into the desiccator again for 30 minutes to 1 hour to make sure that there are no air bubbles inside the PDMS. Subsequently, the mold with PDMS was put into the incubator (Memmert, GmbH) at 65 ° C for at least 2 hours.

After PDMS was cured, the mold was separated into three pieces and PDMS has been removed from the mold with the help of tweezers as it can be seen in below Figure 3.7 and Figure 3.8.

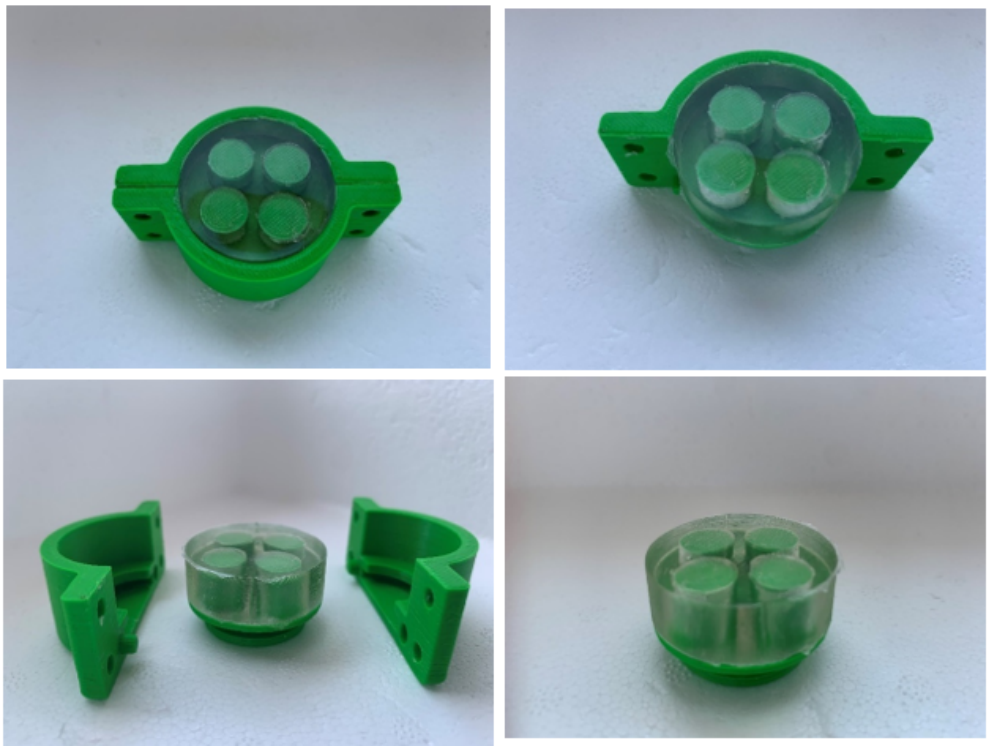

Figure 3.7 PDMS substrate in the mold.

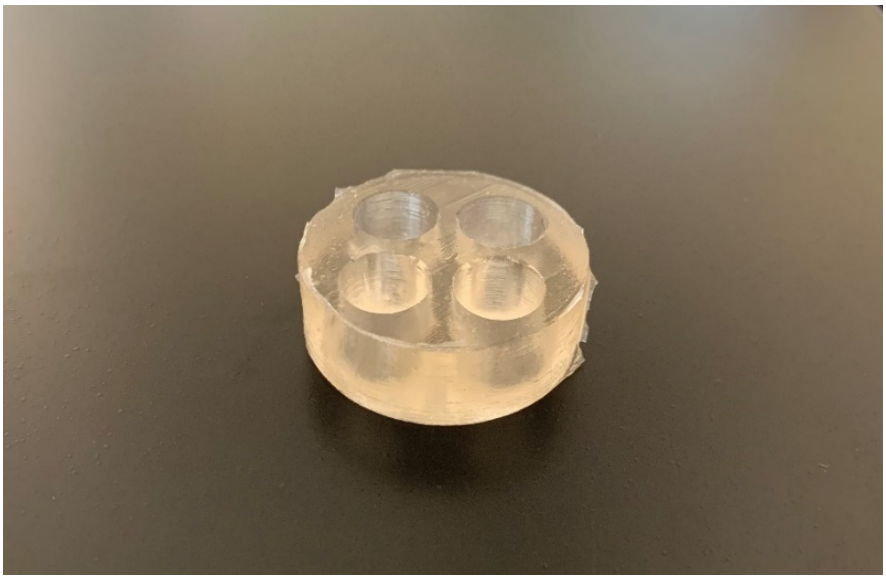

Figure 3.8 Cured PDMS.

3.2 NiTi Surfaces

NiTi surfaces have been cut circularly by a clipper with a diameter of 11 mm from the NiTi plate. Then, these NiTi surfaces have been placed into each well of PDMS substrates as shown in below Figure 3.9.

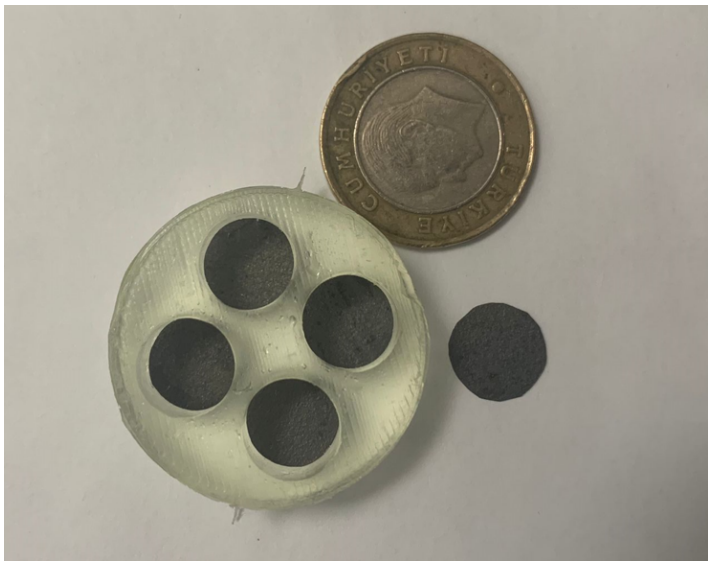

Figure 3.9 NiTi surfaces placed into the PDMS substrate.

3.3 Sterilization

All PDMS substrates, NiTi surfaces, and the other test equipment such as tweezers have been sterilized before initiating the experiments. The sterilization process has begun with the NiTi surfaces sterilization. Firstly, NiTi surfaces have been sterilized by using Ultra Gold ultrasonic cleaner (Hydra Ultrasonic, Turkey) at 45°C with 95.9 % ethanol absolute (Tekkim Kimya, Turkey) for 5 minutes, the acetone (Honeywell International Inc, Charlotte, North Carolina, US) for 5 minutes, and 70% Ethylene Oxide (EtO) which was obtained by diluting 95.9% ethanol absolute (Tekkim Kimya, Turkey) for 5 minutes, respectively. Afterwards, NiTi plates and PDMS substrates were sterilized into the autoclave machine (NÜVE OT 40L, Turkey) for 20 minutes at 134°C. Then, all sterile samples have been placed into the class II biological safety cabinet (ESCO Life Sciences Group, Singapore). NiTi surfaces have been located into each well of PDMS substrates in the flow hood. 300 µl 70% EtO solution was put into each well with NiTi surfaces for 15 minutes. After that, EtO solution was aspirated and this step was repeated again. Hereby, the sterilization process of all samples has been accomplished.

3.4 Ultrasound Application

Ultrasound application has been performed on each PDMS substrate after 24 hours of cell culture cultivation on NiTi surfaces by 1631903 Sonopuls 190 (Enraf Nonius, Holland). There are 7 application groups given in Table 3.1 Ultrasound has been applied in continuous mode at 3 different intensities and 2 different frequency amplitudes.

Table 3.1
Application Groups and Parameters

Application Groups	Intensity [W/cm^2]	Frequency [MHz]
Group I	0.2	1
Group II	0.2	3
Group III	0.5	1
Group IV	0.5	3
Group V	0.75	1
Group VI	0.75	3
Group VII-Control	Not Applied	Not Applied

A head holder which has 5 cm^2 surface area has been used. Before the sonication, the holder was fixed and the surface of the fixed holder has been covered by 2 ml contact–gel (Aqua Ultrasound Gel, Neo Kurumsal, Turkey). Each PDMS substrate has been sealed to the sterile lip in the flow hood and then located on the holder with the contact-gel and exposed to ultrasound application for 2 minutes from the bottom of the PDMS substrate shown in below Figure 3.10.

Figure 3.10 Ultrasound Application.

After the application, the temperature of each PDMS substrate has been measured by an infrared thermometer (Xidian F002 Forehead Thermometer) as shown in below Figure 3.11. The temperature values were measured from the bottom of the substrate and all values were recorded. Then, all samples were kept in the incubator for 1 day at 37°C for L929 mouse fibroblasts and MCF-7 human breast cancer cells.

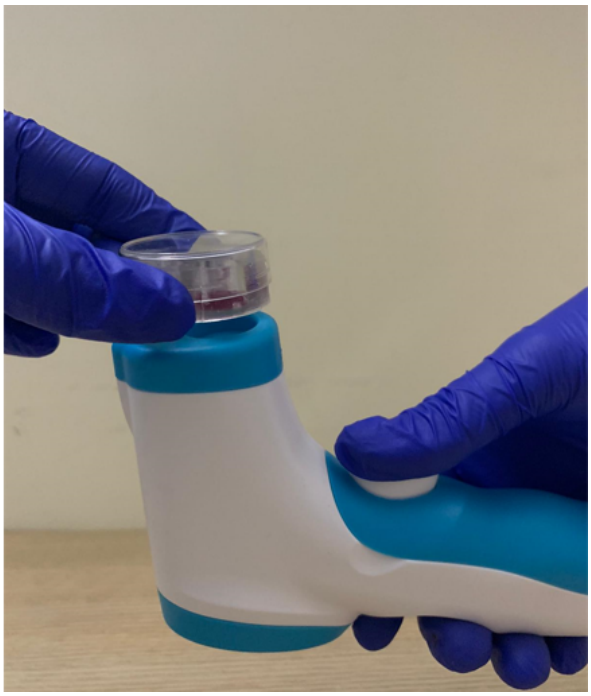

Figure 3.11 Temperature Measurement.

3.5 Cell Culture Studies

L929 mouse fibroblast cells were routinely cultured in 25 cm^2 flasks (SARSTEDT AG & Co. KG, Nümbrecht, Germany) with Dulbecco's Modified Eagle's Medium (DMEM) High Glucose (Biosera, Nuaille, France), supplemented with 10% Fetal Bovine Serum (FBS) (ATCC® 30-200TM) and 1% peniciline-streptomycin (Biosera, Nuaille, France), and kept in a humified 5% carbon dioxide (CO^2) atmosphere at 37°C.

Similar to L929 fibroblast cells, MCF-7 human breast cancer cell lines were routinely cultured in 25 cm^2 flasks with DMEM F-12 (Biosera, Nuaille, France), supplemented with 10% FBS (ATCC® 30-200TM), and 1% peniciline-streptomycin (Biosera,

Nuaille, France), and kept in a humified 5% CO^2 atmosphere at 37°C. The NiTi surface area is 95 mm^2 and the cell density of L929 fibroblasts and MCF-7 breast cancer cell lines has been determined as 5x104 cells/ml for each NiTi. Once the adequate number of cells have been obtained, the cell cultures have been cultivated in NiTi surfaces with 300 µl working volume of medium.

3.5.1 Alamar Blue (AB) Cell Viability Assay

In order to enquire cellular viability after the ultrasound application, the Alamar Blue (AB) Cell Viability Assay has been performed at particular time points. For this purpose, firstly, AB assay (Bio-Rad Laboratories, Inc) was prepared by mixing the fresh medium and AB dye at the ratio of 10:1. Afterwards, the cell culture medium has been replaced by 300 µl, 10% AB solution and then incubated for three hours. It has been performed after 24 and 48 hours of the cell culture. At the end of three hours, 100 µl AB solution has taken from each well and put into the 96-well plate for the measurement of the absorbance values at 570 nm and 595 nm in 96-well plate reader (iMarkTM Microplate Absorbance Reader, Bio-Rad Laboratories, Inc,). After the mix time was entered as 3 seconds, and the mix speed was arranged as low, the measurement has been performed and the absorbance values have been recorded.

3.5.2 Acridine Orange (AO) and Propidium Iodide (PI) Staining for Cell Viability

Firstly, the stock solutions have been prepared by dissolving 5 mg/ml AO (Sigma Aldrich, Germany) and 3 mg/ml PI (Glentham Life Sciences, UK) in basic ethanol. Then, the staining solutions have been developped by mixing the stock solutios and phosphate buffered saline (PBS) at the ratio of 1:1000. After the second AB cellular viability assay has been performed, AB solution was aspirated from each well and 300 µl fresh medium was added. For AO/PI cell viability test, two 2 out of 4 wells of each PDMS substrates were practiced. After the aspiration of 300 µl medium, NiTi

surfaces have been washed with 250 µl PBS solution twice. Then, 100 µl AO and 100 µl PI was added to each well. Samples were gently shaked for 1 minute. Afterward, NiTi surfaces were ejected from the PMDS substrates and put under the fluorescent microscope (Leica DM IL LED; Leica Microsystems) to display the cells.

3.5.3 Immunofluorescence staining with 4', 6–diamidino–2–phenylindole (DAPI) and F–actin

Prior to the immunofluorescence staining, the cell fixation process should be performed. The living cells on the remaining two NiTi surfaces of each PDMS substrate were fixed with 4% paraformaldehyde solution (PFA) (Sigma Aldrich, Germany) for 10 minutes and then permeabilized with 1% tritonX-100 (Sigma Aldrich, Germany) solution for 10 minutes. Nonspecific binding of phallotoxin was blocked with 1% Bovine Serum Albumin (BSA) (Biosera, Nuaille, France) solution for 30 minutes.

After cell fixation, the staining solution of Phalloidin-iFluor 488 reagent has been prepared by diluting it in PBS and 1% BSA at the ratio of 1:1000. Then, 100 µl staining solution was added to the remaining 2 wells and samples were gently shaked for at least 20 minutes to observe the actin cytoskeletons of cells. Then, Phalloidin-iFluor was aspirated and cells have been washed 250 µl PBS twice. Hereafter, 100 µl DAPI counterstaining (Thermo Fisher Scientific) was added and the samples were gently shaked for 5 minutes for labelling of the nuclei.

4. RESULTS

PDMS substrates with flat NiTi surfaces were prepared to simulate the implantable vascular nitinol stents. Then, ultrasound application has been performed to cell lines cultured on NiTi surfaces. The effects of the ultrasound application in terms of the cellular viability have been evaluated in this chapter.

4.1 Cell Viability Assay

The ultrasound effect on cell lines was examined by Alamar Blue (AB) Cell Viability Assay. L929 fibroblast cells, and MCF-7 human breast cancer cells were cultured on NiTi surfaces and tissue culture polystyrene (TCP) plates. To evaluate the cell viability, AB assay was used after the first and second day of ultrasound application. Additionally, after the ultrasound application, the temperature value of each PDMS substrate has been measured and recorded to evaluate the temperature effect owing to ultrasound exposure to the cell viability. The results of AB assay for each cell have been statistically analyzed by GraphPad Prism 9. For this purpose, the Kruskal-Wallis analysis was performed.

L929 fibroblast cell results were shown in below Figure 4.1. As a result of the statistical analysis, there is no significant difference ($p=0.694$, Kruskal-Wallis statistic value, $H=4.721$) between day 1 and day 2. Therefore, it can be concluded that ultrasound application has no negative effect regarding the cellular viability. Also, it was proven that there is no toxic effect due to NiTi surfaces. Cellular activity on NiTi surfaces has been maintained after the sonication.

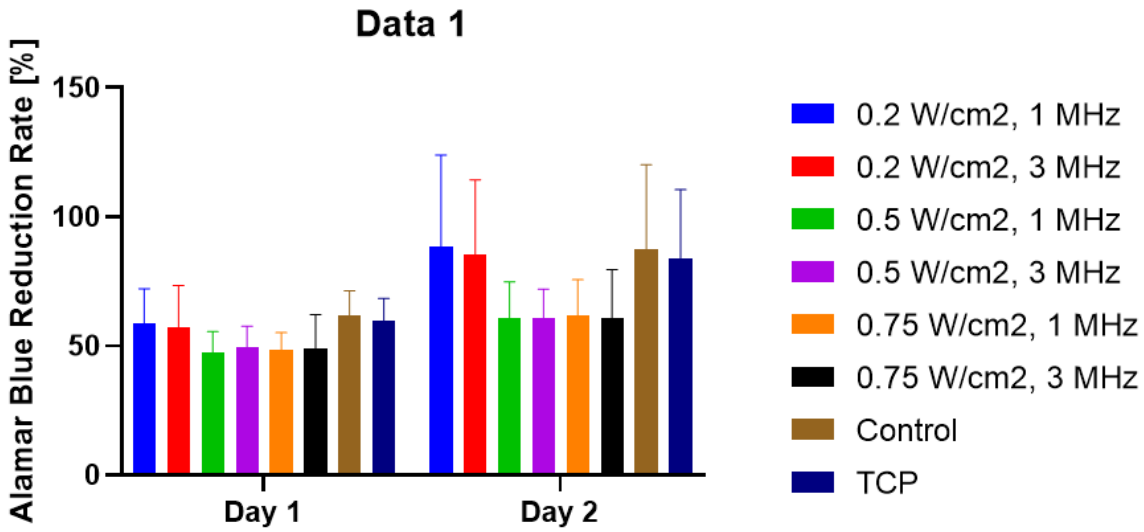

Figure 4.1 AB Reduction Rates of Fibroblasts.

Moreover, the cellular viability can be evaluated in terms of the temperature effect. Since the ultrasound may cause heat-induced damage to cells at high frequencies and/or high intensities, it was achieved to preserve cell viability by controlling the temperature after the application. Due to the ultrasound exposure, the temperature value of the samples can be changed. For fibroblast cell line, the recorded temperature values are given below Table 4.1. It was obvious that the temperature was increased at high intensities compared to lower ones.

Table 4.1
Temperature Results of Fibroblasts

Application Groups	**Temperature Results**
Group I, 0.2 W/cm^2, 1 MHz	30.8°C
Group II, 0.2 W/cm^2, 3 MHz	34.0°C
Group III, 0.5 W/cm^2, 1 MHz	38.1°C
Group IV, 0.5 W/cm^2, 3 MHz	35.2°C
Group V, 0.75 W/cm^2, 1 MHz	40.9°C
Group VI, 0.75 W/cm^2, 3 MHz	40.2°C

As a result of the AB cell viability assay, the cell viability has been increased at day 2 for all dosages. Furthermore, the highest result was observed at low intensities, 0.2 W/cm^2 compared to the other dosages. Also, the lowest temperature values have been measured after the ultrasound exposure at low intensities for fibroblast cells. Therefore, it was proven that the fibroblast cell lines can preserve their metabolic activity after the low-intensity ultrasound application at low temperatures.

For MCF-7 human breast cancer cells, the results were given in below Figure 4.2. Based on the statistical analysis, there is no significant difference (p=0.7101, H=4.588) among day 1 and day 2. Therefore, it can be resolved that the cellular viability has been retained after the sonication. Additionally, there is no adverse event regarding the metabolic activity of cells due to the NiTi surfaces.

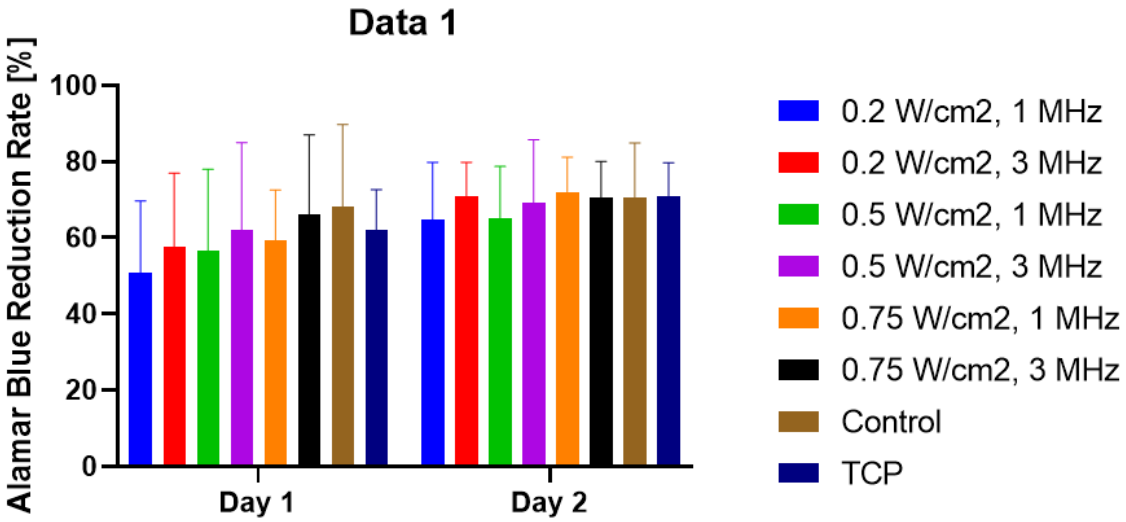

Figure 4.2 AB Reduction Rates of MCF-7 Cells.

Besides, the temperature values of MCF-7 cells are given in below Table 4.2. Similar to fibroblast cells, the cell viability has been mostly increased at low densities for MCF-7 human breast cancer cells at low temperatures.

Even if the test samples have been incubated at 37°C, the ultrasound application have been performed in the room temperature which is around 20-22°C. That's why the temperature values can be decreased after the ultrasound application as it can

be seen in the lower intensities. However, this temperature decrease has no negative impact on the cellular viability for MCF-7 cells.

Table 4.2
Temperature Results of Fibroblasts

Application Groups	Temperature Results
Group I, 0.2 W/cm^2, 1 MHz	29.5°C
Group II, 0.2 W/cm^2, 3 MHz	29.7°C
Group III, 0.5 W/cm^2, 1 MHz	31.8°C
Group IV, 0.5 W/cm^2, 3 MHz	35.0°C
Group V, 0.75 W/cm^2, 1 MHz	38.3°C
Group VI, 0.75 W/cm^2, 3 MHz	39.9°C

4.1.1 AO/PI Staining

Images taken from AO/PI-stained cells cultured on NiTi surfaces as shown in below Table 4.3. The living cells are clearly visible in the first column while the dead cells can be seen in the second column. The merged images are put in the third column.

Compared to TCP as an ideal environment, the distribution of the cells on NiTi is mostly homogeneous. Cells exposed to ultrasound have been covered almost all NiTi surfaces by proliferation. Moreover, fibroblast cells on NiTi and TCP are very similar regarding the cell structure. There is no deformation observed due to NiTi. It has been preserved as shown in below figures.

Additionally, cell viability was compared among the cells exposed to ultrasound and the control group for the evaluation of ultrasound impact. There is no negative influence on cells for all dosages. As a result of the ultrasound application, cell proliferation and viability is higher at low intensities for both 1 MHz and 3 MHz frequencies for fibroblast cells. For example, cell proliferation is higher at 0.2 W/cm^2. Also, the number of dead cells have been obtained more at high intensity ultrasound. Thus,

fibroblast cell vitality can be preserved and retained concerning the impacts of the ultrasound application and NiTi.

Figure 4.3 AO/PI Staining Results of Fibroblasts.

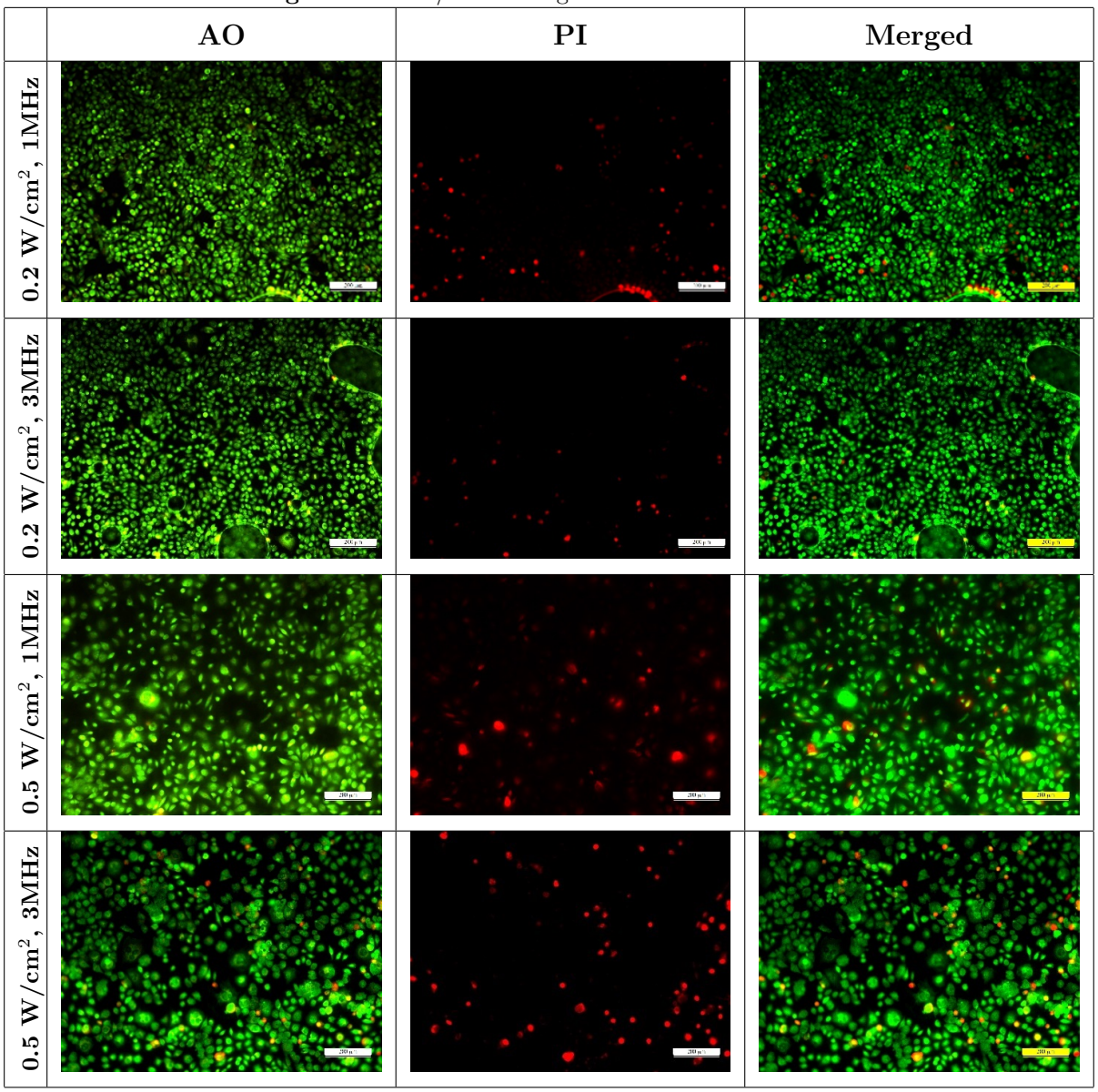

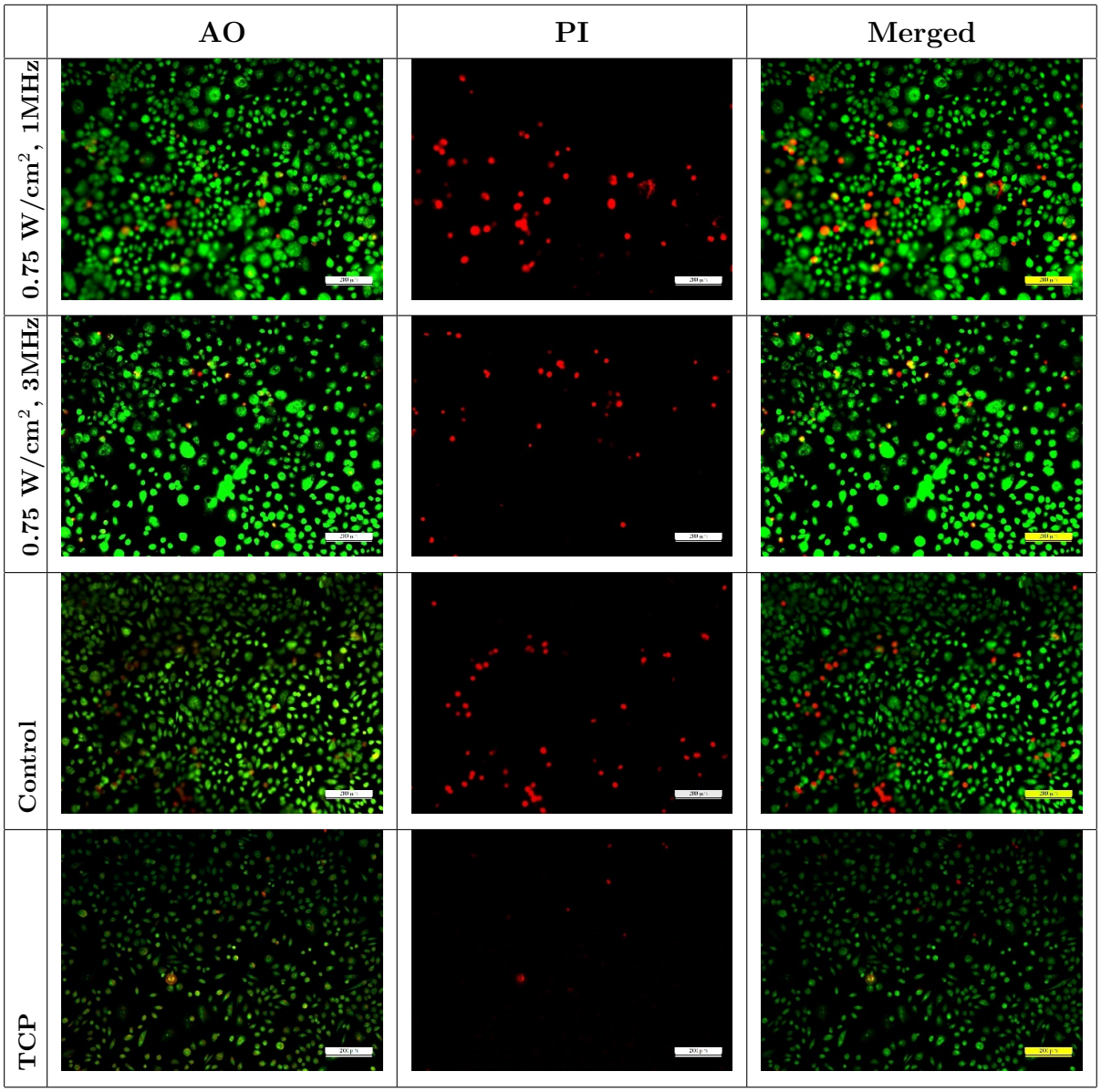

In order to evaluate the cellular viability of MCF-7 cells, AO/PI staining images have been taken. As it can be seen in below Table 4.4., MCF-7 cell structure has not been damage after they were seeded on NiTi.

The cell growth should be prevented and/or kept under control during the routine treatment of the breast cancer. The cellular viability is higher on TCP, is an ideal place for the cell growth, compared to NiTi surfaces as shown in below figures. Therefore, it was proven that NiTi as a biomaterial has contribute to control the MCF-7 cancer cell growth.

Also, regarding the ultrasound effect, MCF-7 cells exposed to the ultrasound and control group was compared. Ultrasound can support to inhibit cell generation on NiTi. It can prevent faster proliferation of the cancer cells based on the AO/PI staining images below.

Figure 4.4 AO/PI Staining Results of MCF-7 Cells.

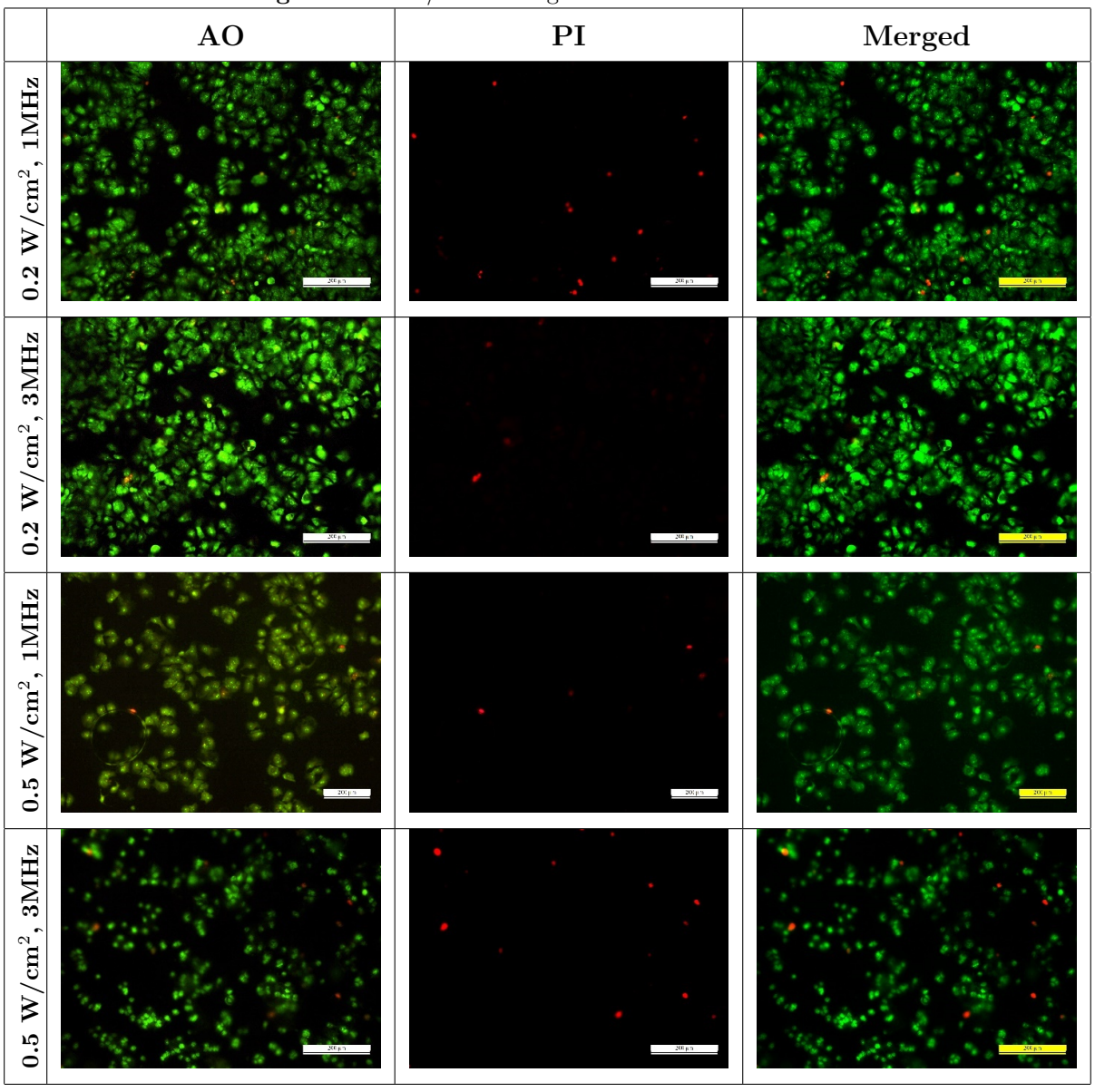

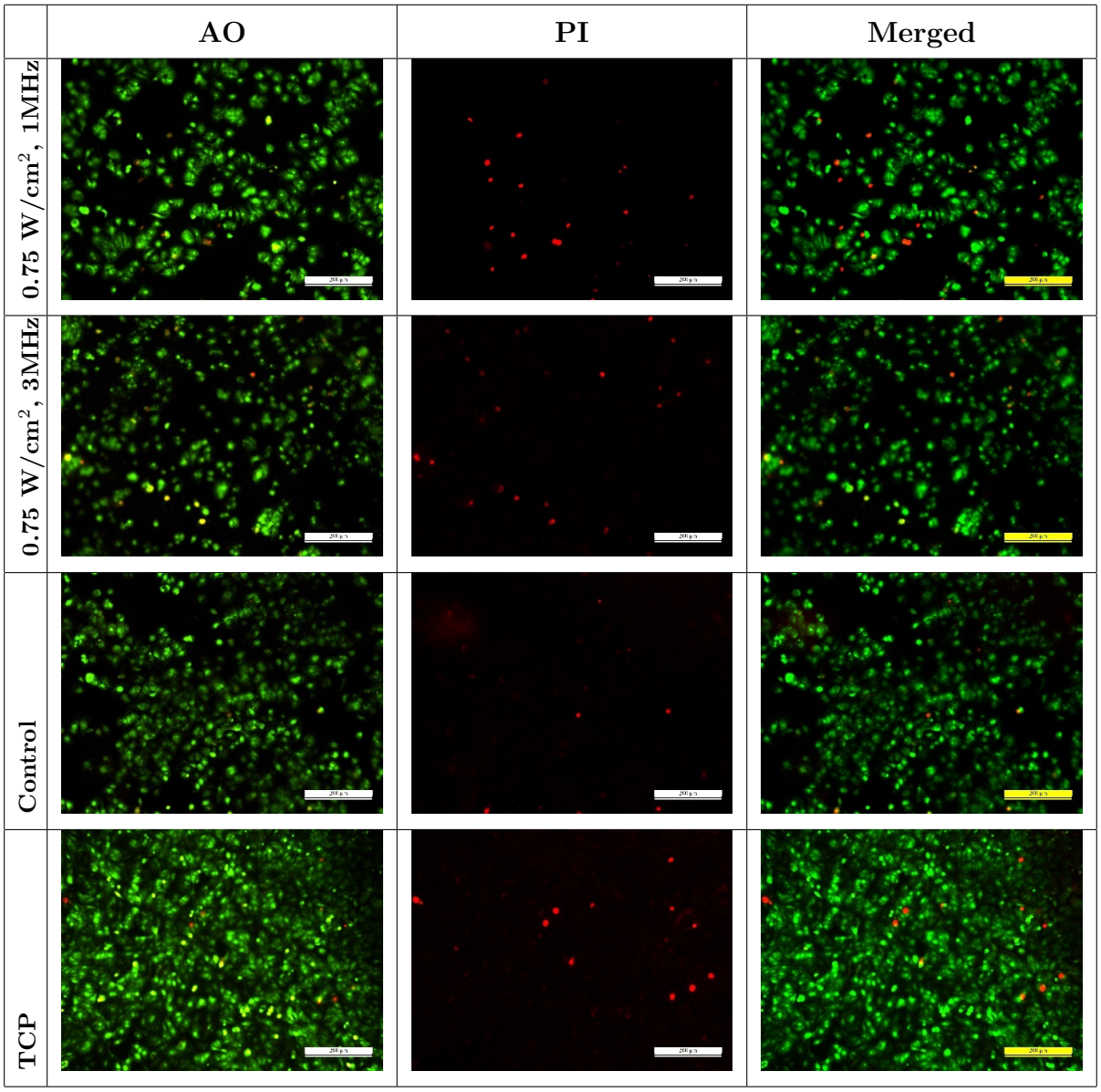

4.1.2 Immunostaining with F-actin/DAPI

Images of F-actin and DAPI stained fibroblast and MCF-7 cells have been taken as shown in Table 4.5. and 4.6. Thanks to Phalloidin- iFluor 488 Reagent, F-actin filaments of the living cells are clearly visible in the first column. Also, DAPI were used to dye cell nuclei of the living and fixed cells as shown in the second column. The cellular viability can be observed in below figures.

Compared to TCP and other samples for the evaluation of the impact of NiTi surface, there is no obvious difference for the distribution and/or the structure of

the cells. Therefore, it can be accepted that NiTi has no negative impact on the cell viability of fibroblast cell line. Also, the ultrasound effect can be evaluated by the comparison the images taken from fibroblast cells which have been exposed to ultrasound waves and the control group. There is no significant differences as it can be seen in below images. Hereby, it was proven that the ultrasound application and using NiTi as a biomaterial have not been induced any necrosis and deformation on the fibroblast cell structure.

Figure 4.5 Immunostaining with F-actin/DAPI.

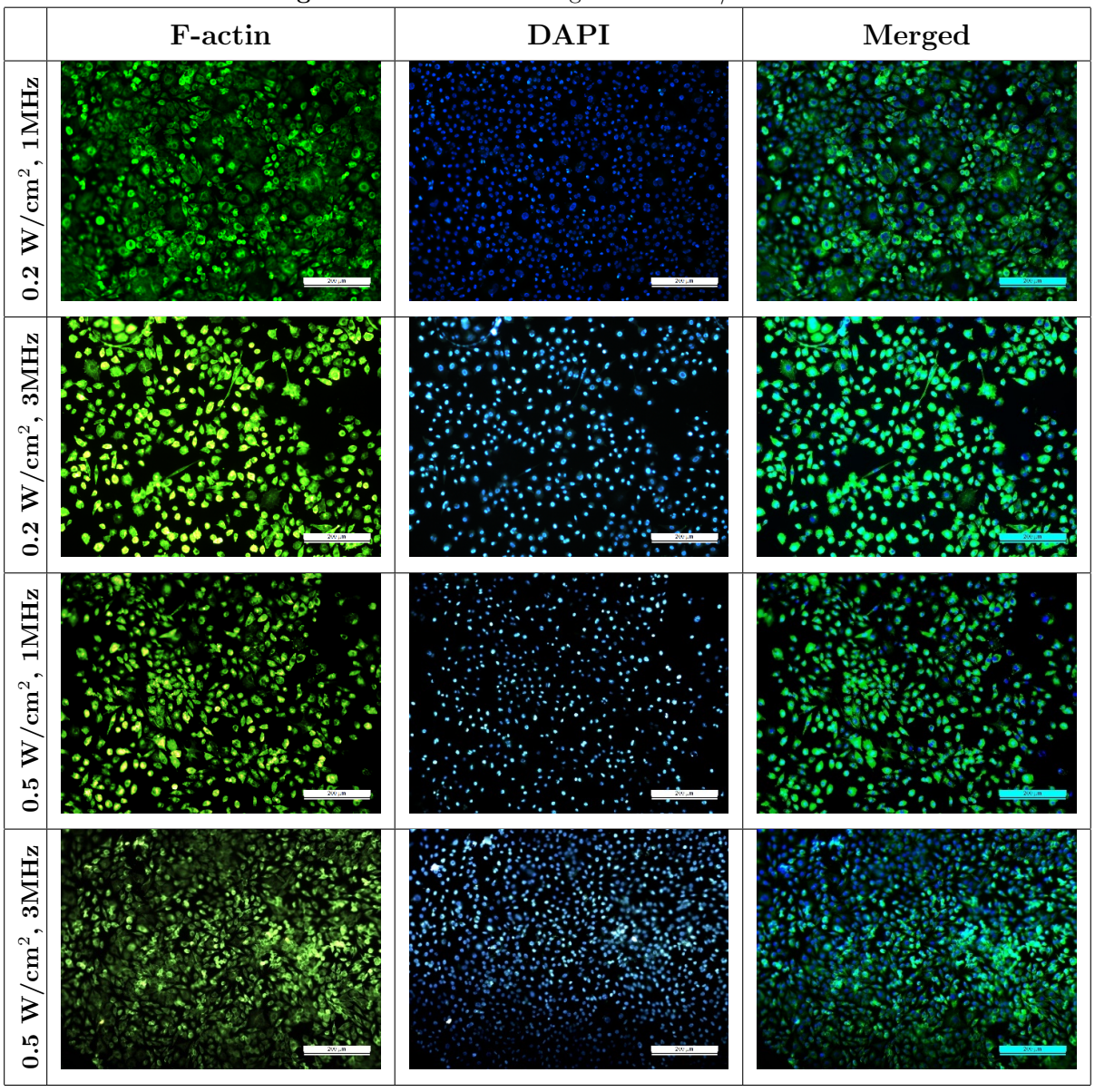

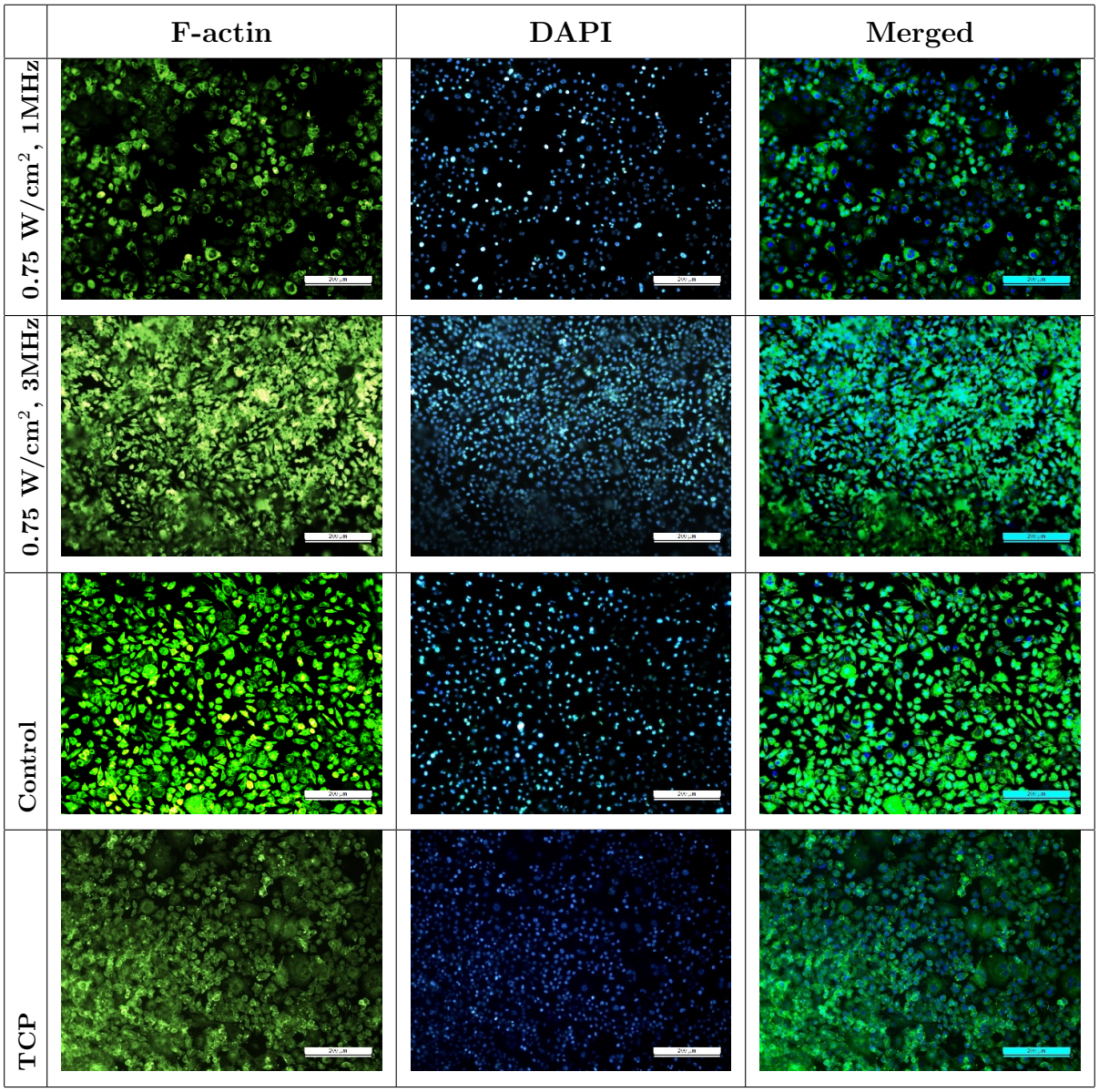

For MCF-7 human breast cancer cell line, F-actin and DAPI stained has been utilized as well. The cytoskeleton of the cells was clearly visible for each sample as shown in the first column. Also, the nuclei of MCF-7 cells can be detected distinctly in the second column.

Figure 4.6 Immunostaining with F-actin/DAPI.

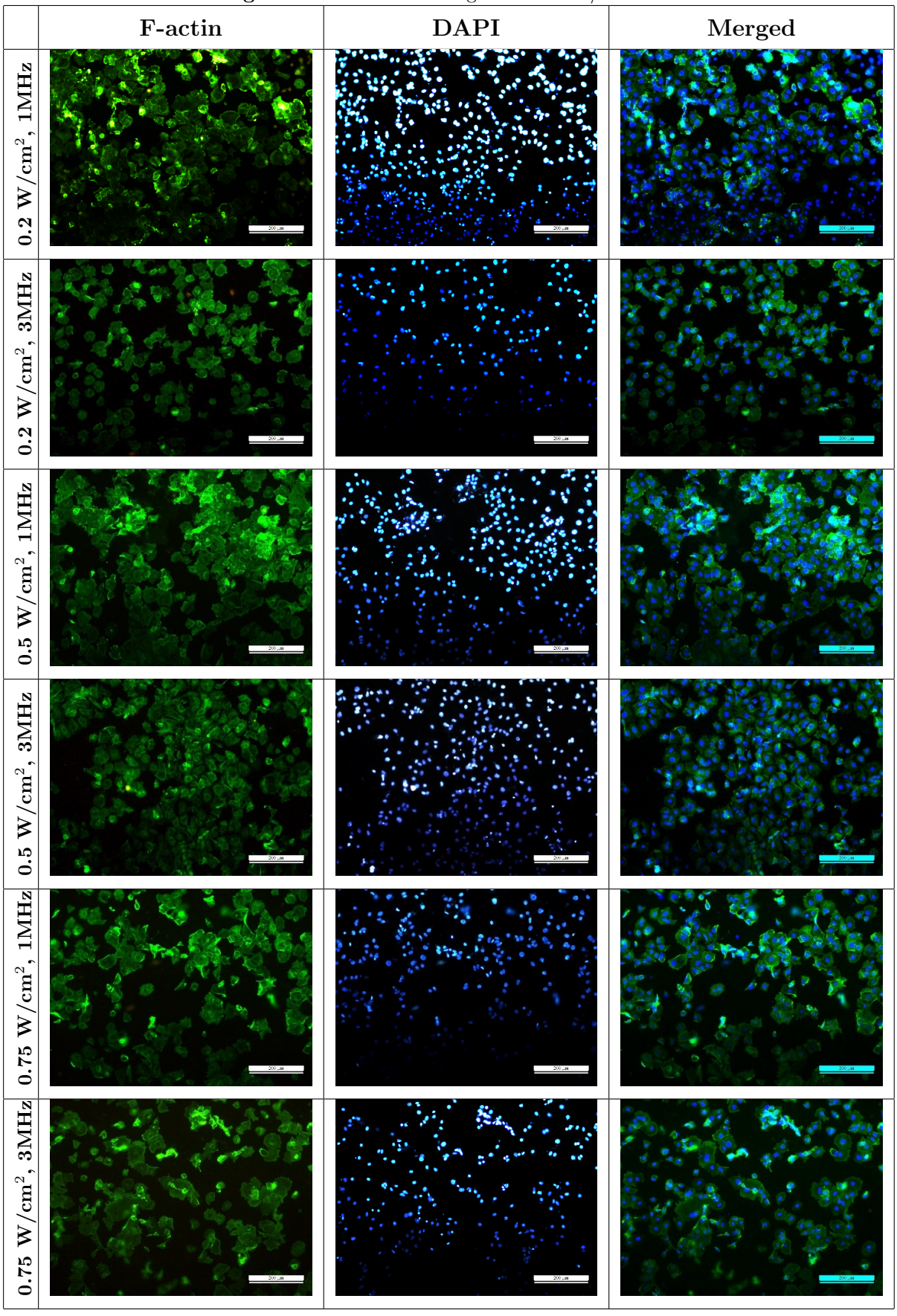

	F-actin	DAPI	Merged
Control	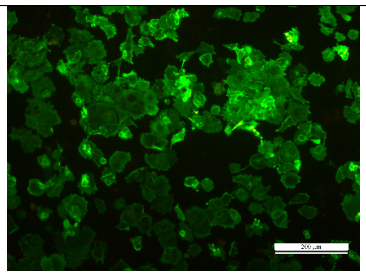	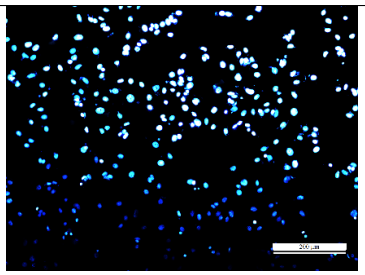	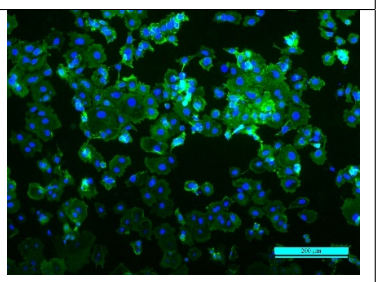
TCP	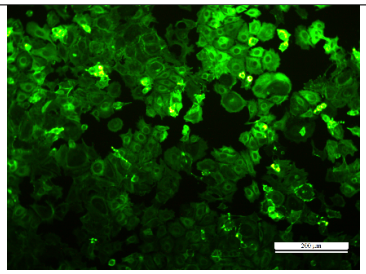	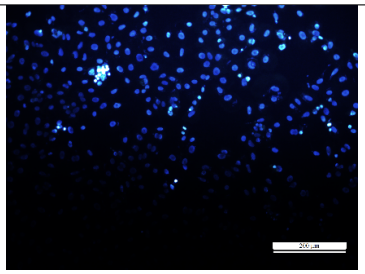	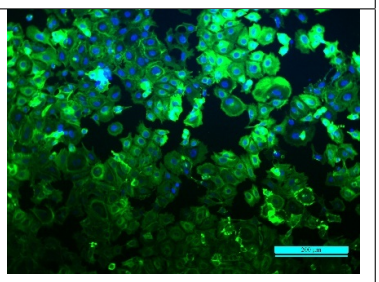

5. DISCUSSION

Especially for the percutaneously implanted, permanent medical devices such as vascular stents, the immune system response to the implant device should be considered strongly. In order to prevent any adverse events after the implantation, the cell viability and endothelial cells proliferation are crucial. To enhance the endothelization speed on the implant surface, two main criteria can be evaluated regarding the design and fabrication of the implantable medical devices. One of them is using highly biocompatible material such as nitinol. The other one can be applying the feasible therapeutic approach like ultrasound.

Many of the research results showed that different cell lines can be impacted by ultrasound regarding the cell viability. In order to investigate the effects of ultrasound, it has been performed at different dosages for continuous and pulsed mode in a lot of studies. Therefore, for L929 mouse fibroblast cell line, the findings can reveal that the ultrasound application can enable to raise cell viability and prevent the cell damage at low intensities comparing to the high intensities [7, 11, 12, 14, 18, 19]. In this thesis, our results are also revealed that the highest cell viability is observed at low intensities and low frequencies, 0.2 W/cm^2, 1 MHz and 0.2 W/cm^2, 3 MHz in comparison with the high intensities.

Additionally, for MCF-7 human breast cancer lines, ultrasound therapy has been applied to stimulate necrosis and/or prevent to cell growth. Researches indicated that ultrasound can clearly affect MCF-7 cell growth at different intensities. For instance, Wu et.al. [29] and Peek et.al. [25] claimed that applying high intensity focused ultrasound (HIFU) can lead to necrosis and severe damage for MCF-7 cells. On the other hand, it was observed that MCF-7 cell lines has been damaged at low intensities as well [22, 23]. As a result of these researches, it can be concluded that ultrasound therapy can induce the cell growth of MCF-7 cell lines at both low and high intensities. According to our results, the cell growth can be inhibited by performing ultrasound

to MCF-7 cell lines. Based on our findings, there is no significant difference among the cell viability results at day 1 and day 2. Therefore, it can be claimed that the ultrasound therapy can be utilized to control the cell growth while cellular viability is maintained.

6. CONCLUSION

Vascular stents are widely used to treat atherosclerosis, is an artery obstruction, is a common cardiovascular disease. However, vascular stents are prone to restenosis. After the implantation of the stent, new, innovative, and non-invasive approaches such as ultrasound application can be performed to inhibit thrombus formation, in-stent restenosis, and improve endothelization. Carotid stents can be a great candidate for the ultrasound applications because they are superficial and easier to target during the ultrasound applications.

For this purpose, in this thesis, the ultrasound has been applied to L929 mouse fibroblast cells and MCF-7 human breast cancer cells, which are seeded on NiTi surfaces placed into the PDMS substrates. PDMS can represent the vessel structure and NiTi can behave as a stent deployed in the vessel. Afterward, ultrasound was exposed to the target cells on NiTi to simulate the in-vivo conditions.

By applying different dosages of ultrasound, the impact of sonication has been evaluated regarding cellular viability and endothelization accordingly. As a representative work of ultrasound exposure to NiTi-based stents after the implantation procedure, two different cell lines have been utilized. For the preliminary examination, fibroblast cells which have a major role in the tissue repair process have been chosen. It was aimed to maintain cell viability and growth after the ultrasound. It has been performed at 6 different dosages and the highest viability for the fibroblast cells has been observed at low intensities; 0.2 W/cm^2, 1 MHz, and 0.2 W/cm^2, 3 MHz.

In addition to fibroblast cells, MCF-7 human breast cancer cells have been selected to see the different impacts of ultrasound because it is very crucial to inhibit cell growth and/or observe the necrosis of cancer cells. Based on our findings, there is no significant difference in cell proliferation after ultrasound exposure. Therefore, it can be concluded that ultrasound therapy can help to control the growth of the MCF-7

cells.

As a consequence of this first assessment, it was proven that ultrasound can impact cell viability and proliferation since it has been applied to different cell lines to detect the cellular activity on NiTi surfaces. While ultrasound can provide the cell proliferation for fibroblast cells, it can help to control and inhibit cell growth for MCF-7 cells. Therefore, it can be a representative and promising study to investigate the effect of ultrasound both to observe endothelization and to prevent cell proliferation that causes atherosclerosis.

7. FUTURE WORKS

In this thesis, the results revealed that ultrasound therapy can induce cellular viability. It is a promising method to obtain faster endothelization and prevent vessel occlusion.

Further prospective studies will be conducted by applying repetitive ultrasound to different cell lines such as carotid artery cells, or endothelial cells. More ultrasound dosages in terms of various intensities and frequencies in different modes; continuous and pulse modes, will be applied to find the appropriate range for the treatment.

Additionally, different stent types can be used to observe the ultrasound effect regarding endothelization. For instance, a comparison study will be performed to evaluate the ultrasound impact on bare metal stents and/or covered stents.

Furthermore, ultrasound therapy can be used with some other innovational approaches such as microfluidic systems. Since microfluidics provides an opportunity to simulate several in-vivo conditions, it can be beneficial to detect ultrasound impact to the dynamic microfluidic systems to mimic the human body environment such as blood circulation.

REFERENCES

1. Balbay, G.-A. I., Yücel, S. Malhan and et al, "Modeling the burden of cardiovascular disease in Turkey", *Anatolian Journal of Cardiology*, Vol. 20, No. 4, p. 235, 2018.

2. Organization, W. H., *Cardiovascular Diseases*, 2021, https://www.who.int/health-topics/cardiovascular-diseases#tab=tab_1/, Accessed Sep 2021.

3. Nazneen, F., G. Herzog, D. W. Arrigan and et al, "Surface chemical and physical modification in stent technology for the treatment of coronary artery disease", *Journal of Biomedical Materials Research Part B: Applied Biomaterials*, Vol. 100, No. 7, pp. 1989–2014, 2012.

4. Yin, R.-X., D.-Z. Yang and J.-Z. Wu, "Nanoparticle drug-and gene-eluting stents for the prevention and treatment of coronary restenosis", *Theranostics*, Vol. 4, No. 2, p. 175, 2014.

5. Beshchasna, N., M. Saqib, H. Kraskiewicz and et al, "Recent advances in manufacturing innovative stents", *Pharmaceutics*, Vol. 12, No. 4, p. 349, 2020.

6. *Cardiovascular disease statistics*, 2021, https://ec.europa.eu/eurostat/statistics-explained/index.php?title=Cardiovascular_diseases_statistics, Accessed Sep 2021.

7. Libby, P., J. E. Buring, L. Badimon and et al, "Atherosclerosis", *Nat Rev Dis Primers*, Vol. 5, No. 1, p. 56, 08 2019.

8. Kiousis, D. E., T. C. Gasser and G. A. Holzapfel, "A numerical model to study the interaction of vascular stents with human atherosclerotic lesions", *Annals of Biomedical Engineering*, Vol. 35, No. 11, pp. 1857–1869, 2007.

9. Van de Ven, P., J. Beutler, G. Geyskes and et al, "Transluminal vascular stent for ostial atherosclerotic renal artery stenosis", *The Lancet*, Vol. 346, No. 8976, pp. 672–674, 1995.

10. Abou-Chebl, A., Q. Bashir and J. S. Yadav, "Drug-eluting stents for the treatment of intracranial atherosclerosis: initial experience and midterm angiographic follow-up", *Stroke*, Vol. 36, No. 12, pp. e165–e168, 2005.

11. Liu, Y., J. Yang, Y. Zhou and J. Hu, "Structure design of vascular stents", *Multiscale Simulations and Mechanics of Biological Materials*, pp. 301–317, 2013.

12. Kolodgie, F. D., G. Nakazawa, G. Sangiorgi and et al, "Pathology of atherosclerosis and stenting", *Neuroimaging Clinics of North America*, Vol. 17, No. 3, pp. 285–301, 2007.

13. Ross, R., "Cell biology of atherosclerosis", *Annual Review of Physical Chemistry*, Vol. 57, pp. 791–804, 1995.

14. Bennett, M. R., S. Sinha and G. K. Owens, "Vascular smooth muscle cells in atherosclerosis", *Circulation Research*, Vol. 118, No. 4, pp. 692–702, 2016.

15. Lusis, A. J., "Atherosclerosis", *Nature*, Vol. 407, No. 6801, pp. 233–241, Sep 2000.

16. Memiç, K., *Koroner arter bypass cerrahisi yapılan hastalarda kardiyovasküler risk faktörleri ve koroner ateroskleroz ciddiyetinin uzun dönem greft açıklık oranına etkisi*, 2011, `http://acikerisim.demiroglu.bilim.edu.tr:8080/xmlui/handle/11446/207`, Accessed Sep 2021.

17. Nakazawa, G., S. K. Yazdani, A. V. Finn and et al, "Pathological findings at bifurcation lesions: the impact of flow distribution on atherosclerosis and arterial healing after stent implantation", *Journal of the American College of Cardiology*, Vol. 55, No. 16, pp. 1679–1687, 2010.

18. Hopf-Jensen, S., M. Leissner, L. Marques and et al, "Micromesh Dual-Layer Technology for Carotid Artery Stents", *Vascular Disease Management*, Vol. 13, No. 10, pp. E222–E229, 2016.

19. Derdeyn, C. P. and M. I. Chimowitz, "Angioplasty and stenting for atherosclerotic intracranial stenosis: rationale for a randomized clinical trial", *Neuroimaging Clinics of North America*, Vol. 17, No. 3, pp. 355–363, 2007.

20. Dzau, V. J., R. C. Braun-Dullaeus and D. G. Sedding, "Vascular proliferation and atherosclerosis: new perspectives and therapeutic strategies", *Nature medicine*, Vol. 8, No. 11, pp. 1249–1256, 2002.

21. Giacoppo, D., G. Gargiulo, P. Aruta and et al, "Treatment strategies for coronary in-stent restenosis: systematic review and hierarchical Bayesian network meta-analysis of 24 randomised trials and 4880 patients", *Bmj*, Vol. 351, 2015.

22. Maisel, W. H. and W. K. Laskey, "Drug-eluting stents", *Circulation*, Vol. 115, No. 17, pp. e426–e427, 2007.

23. Victor, A., J. Ribeiro and F. F. Araújo, "Study of PDMS characterization and its applications in biomedicine: A review", *Journal of Mechanical Engineering and Biomechanics*, Vol. 4, No. 1, pp. 1–9, 2019.

24. Chen, A. I., M. L. Balter, M. I. Chen and et al, "Multilayered tissue mimicking skin and vessel phantoms with tunable mechanical, optical, and acoustic properties", *Medical Physics*, Vol. 43, No. 6Part1, pp. 3117–3131, 2016.

25. Liu, J., H. Zheng, X. Dai and et al, "Transparent PDMS Bioreactors for the Fabrication and Analysis of Multi-Layer Pre-vascularized Hydrogels Under Continuous Perfusion", *Frontiers in Bioengineering and Biotechnology*, Vol. 8, 2020.

26. Fiddes, L. K., N. Raz, S. Srigunapalan and et al, "A circular cross-section PDMS microfluidics system for replication of cardiovascular flow conditions", *Biomaterials*, Vol. 31, No. 13, pp. 3459–3464, 2010.

27. Victor, A., J. Ribeiro and F. F. Araújo, "Study of PDMS characterization and its applications in biomedicine: A review", *Journal of Mechanical Engineering and Biomechanics*, Vol. 4, No. 1, pp. 1–9, 2019.

28. Wadood, A., "Brief overview on nitinol as biomaterial", *Advances in Materials Science and Engineering*, Vol. 2016, 2016.

29. Barras, C. and K. Myers, "Nitinol–its use in vascular surgery and other applications", *European Journal of Vascular and Endovascular Surgery*, Vol. 19, No. 6, pp. 564–569, 2000.

30. Pelton, A., D. Stöckel and T. Duerig, "Medical uses of nitinol", *Materials science forum*, Vol. 327, pp. 63–70, Trans Tech Publ, 2000.

31. Trepanier, C., T. Leung, M. Tabrizian and et al, "Preliminary investigation of the effects of surface treatments on biological response to shape memory NiTi stents", *Journal of Biomedical Materials Research: An Official Journal of The Society for Biomaterials, The Japanese Society for Biomaterials, and The Australian Society for Biomaterials*, Vol. 48, No. 2, pp. 165–171, 1999.

32. Derneği, T. T., "Türkiye'de Temel Akciğer Sağlığı Sorunları ve Çözüm Önerileri", *Türk Toraks Derneği Beyaz Kitap. Sentez Matbaacılık ve Yayıncılık, Ankara*, pp. 89–93, 2010.

33. Cleveland Clinic Professionals, *Atherosclerosis: Arterial Disease*, `https://my.clevelandclinic.orghealthdiseases16753atherosclerosis-arterialdisease#atherosclerosis`, Accessed Sep 2021.

34. Beckerman, J., *Atherosclerosis*, 2019, `https://www.webmd.com/heart-diseasewhatisatherosclerosis`, Accessed Sep 2021.

35. Koçak, A., *Karotis Arter ve Periferik Arter Lezyonlarının Değerlendirilmesinde Renkli Doppler Ultrasonografi, Manyetik Rezonans Anjiyografi ve Dijital Substraksiyon Anjiyografi Bulgularının Karşılaştırılması*, 2009.

36. Toutouzas, K., A. Colombo and C. Stefanadis, "Inflammation and restenosis after percutaneous coronary interventions", *European Heart Journal*, Vol. 25, No. 19, pp. 1679–1687, 2004.

37. Davis, N. E., "Atherosclerosis-an Inflammatory Process", *J Insur Med*, Vol. 37, No. 1, pp. 72–75, 2005.

38. Ross, R., "Atherosclerosis—an Inflammatory Disease", *New England Journal of Medicine*, Vol. 340, No. 2, pp. 115–126, 1999.

39. Byrne, R. A., G. W. Stone, J. Ormiston and A. Kastrati, "Coronary Balloon Angioplasty, Stents, and Scaffolds", *The Lancet*, Vol. 390, No. 10096, pp. 781–792, 2017.

40. Bravata, D. M., A. L. Gienger, K. M. McDonald and et al, "Systematic review: The Comparative Effectiveness of Percutaneous Coronary Interventions and Coronary Artery Bypass Graft Surgery", *Annals of Internal Medicine*, Vol. 147, No. 10, pp. 703–716, 2007.

41. Malik, T. F. and V. S. Tivakaran, "Percutaneous Transluminal Coronary Angioplasty", *StatPearls [Internet]*, 2020.

42. Karadağ, B., "Kararlı angina pektoriste girişimsel yaklaşım; koroner anjiyografi ve revaskülarizasyon stratejileri", *İÜ Cerrahpaşa Tıp Fakültesi Sürekli Tıp Eğitimi Etkinlikleri Kardiyoloji Gündemi Sempozyum Dizisi*, Vol. 64, pp. 89–102, 2008.

43. Lee, J. H., E. Do Kim, E. J. Jun and et al, "Analysis of Trends and Prospects Regarding Stents for Human Blood Vessels", *Biomaterials Research*, Vol. 22, No. 1, pp. 1–10, 2018.

44. Butany, J., K. Carmichael, S. Leong and M. Collins, "Coronary Artery Stents: Identification and Evaluation", *Journal of Clinical Pathology*, Vol. 58, No. 8, pp. 795–804, 2005.

45. Al Suwaidi, J., P. B. Berger and D. R. Holmes Jr, "Coronary Artery Stents", *Jama*, Vol. 284, No. 14, pp. 1828–1836, 2000.

46. Dotter, C. T., R. Buschmann, M. K. McKinney and J. Rösch, "Transluminal Expandable Nitinol Coil Stent Grafting: Preliminary Report", *Radiology*, Vol. 147, No. 1, pp. 259–260, 1983.

47. Shimizu, I., A. Wada and M. Sasaki, "A Study on Designing Balloon Expandable Magnesium Alloy Stent for Optimization of Mechanical Characteristics", *Multidisciplinary Digital Publishing Institute Proceedings*, Vol. 2, p. 523, 2018.

48. Bedair, T. M., M. A. ElNaggar, Y. K. Joung and et al, "Recent Advances to Accelerate Re-endothelialization for Vascular Stents", *Journal of Tissue Engineering*, Vol. 8, 2017.

49. Qi, P., S. Chen, T. Liu and et al, "New Strategies for Developing Cardiovascular Stent Surfaces with Novel Functions", *Biointerphases*, Vol. 9, No. 2, p. 029017, 2014.

50. Zhang, Q., Y. Shen, C. Tang and et al, "Surface Modification of Coronary Stents with SiCOH Plasma Nanocoatings for Improving Endothelialization and Anticoagulation", *Journal of Biomedical Materials Research Part B: Applied Biomaterials*, Vol. 103, No. 2, pp. 464–472, 2015.

51. Modi K, M. K., Soos MP, *Stent Thrombosis*, 2021, https://www.ncbi.nlm.nih.gov/books/NBK441908/, Updated 2021 Jul 31.

52. Elieson, M., T. Mixon and J. Carpenter, "Coronary Stent Infections: A Case Report and Literature Review", *Texas Heart Institute Journal*, Vol. 39, No. 6, p. 884, 2012.

53. Camenzind, E., P. G. Steg and W. Wijns, "A Cause for Concern", *Circulation*, Vol. 115, No. 11, pp. 1440–1455, 2007.

54. Buccheri, D., D. Piraino, G. Andolina and B. Cortese, "Understanding and managing in-stent restenosis: a review of clinical data, from pathogenesis to treatment", *J Thorac Dis*, Vol. 8, No. 10, pp. E1150–E1162, Oct 2016.

55. Nakamura, K., J. H. Keating and E. R. Edelman, "Pathology of Endovascular Stents", *Interv Cardiol Clin*, Vol. 5, No. 3, pp. 391–403, 07 2016.

56. Lovely Chhabra, M. A. Z. W. J. S., *Coronary Stents*, 2021, https://www.ncbi.nlm.nih.gov/books/NBK507804/, Updated 2021 Jul 31.

57. *REBEL Stent System*, https://www.bostonscientific.com/en-US/products/stents--coronary/rebel-platinum-chromium-coronary-stent-system.html, Accessed Sep 2021.

58. Madjarov, J., *Stents*, 2009, https://www.ctsnet.org/article/stents, Accessed Sep 2021.

59. Kwon, C. I., K. H. Ko, K. B. Hahm and D. H. Kang, "Functional self-expandable metal stents in biliary obstruction", *Clin Endosc*, Vol. 46, No. 5, pp. 515–521, Sep 2013.

60. Ana Echarri Piudo, C. L. A., *1.2.4. Self-Expandable Stents*, http://endoinflamatoria.com/i-2-4-self-expandable-stents/, Accessed Sep 2021.

61. Charlton-Ouw, K. M., M. G. Davies and A. B. Lumsden, "Chapter 25 - Intravascular Stenting in Aortoiliac Arterial Occlusive Disease", W. S. Moore and S. S. Ahn (Editors), *Endovascular Surgery (Fourth Edition)*, pp. 271–284, W.B. Saunders, Philadelphia, fourth edition edn., 2011, https://www.sciencedirect.comsciencearticlepiiB9781416062080100254.

62. Andrew T. Kwa, J. R. L., David L. Dawson, *Covered Stents for Treating Aortoiliac Occlusive Disease*, 2011, https://evtoday.comarticles2011aprcovered-stentsfortreatingaortoiliacocclusivedisease, Accessed Sep 2021.

63. Schächinger, V. and A. M. Zeiher, "Covered stent grafts: role in intervention of coronary arteries and degenerated vein grafts", *Z Kardiol*, Vol. 91 Suppl 3, pp. 58–63, 2002.

64. *Advanta V12*, https://www.getinge.com/tr/product-catalog/advanta-v12-balloon-expandable-covered-stent, Accessed Sep 2021.

65. Lipinski, M. J., R. O. Escarcega, N. C. Baker, H. A. Benn, M. A. Gaglia, R. Torguson and R. Waksman, "Scaffold Thrombosis After Percutaneous Coronary Intervention With ABSORB Bioresorbable Vascular Scaffold: A Systematic Review and Meta-Analysis", *JACC Cardiovasc Interv*, Vol. 9, No. 1, pp. 12–24, Jan 2016.

66. Kereiakes, D. J., Y. Onuma, P. W. Serruys and G. W. Stone, "Bioresorbable Vascular Scaffolds for Coronary Revascularization", *Circulation*, Vol. 134, No. 2, pp. 168–182, Jul 2016.

67. Petrini, L., A. Trotta, E. Dordoni and e. a. Migliavacca, "A Computational Approach for the Prediction of Fatigue Behaviour in Peripheral Stents: Application to a Clinical Case", *Ann Biomed Eng*, Vol. 44, No. 2, pp. 536–547, Feb 2016.

68. Faries, P., N. J. Morrissey, V. Teodorescu and et al, "Recent Advances in Peripheral Angioplasty and Stenting", *Angiology*, Vol. 53, No. 6, pp. 617–626, 2002.

69. Baiu, I. and J. R. Stern, "Carotid Artery Stenting", *JAMA*, Vol. 324, No. 16, pp. 1690–1690, 10 2020, https://doi.org/10.1001/jama.2020.10426.

70. Park, J. H. and J. H. Lee, "Carotid Artery Stenting", *Korean Circ J*, Vol. 48, No. 2, pp. 97–113, Feb 2018.

71. Hiramoto, J. S., M. Teraa, G. J. de Borst and M. S. Conte, "Interventions for lower extremity peripheral artery disease", *Nat Rev Cardiol*, Vol. 15, No. 6, pp. 332–350, 06 2018.

72. Nematzadeh, F. and S. Sadrnezhaad, "Effects of material properties on mechanical performance of Nitinol stent designed for femoral artery: Finite element analysis", *Scientia Iranica*, Vol. 19, No. 6, pp. 1564–1571, 2012, https://www.sciencedirect.com/science/article/pii/S1026309812002350.

73. *Peripheral Vascular Disease*, http://www.vascularpractice.org/Peripheral_Vascular_Disease.html, Accessed Sep 2021.

74. Lederman, R. J., F. O. Mendelsohn, R. Santos and et al, "Primary renal artery stenting: Characteristics and outcomes after 363 procedures", *American Heart Journal*, Vol. 142, No. 2, pp. 314–323, 2001, https://www.sciencedirect.com/science/article/pii/S0002870301103145.

75. Cooper, C. J. and T. P. Murphy, "Is renal artery stenting the correct treatment of renal artery stenosis? The case for renal artery stenting for treatment of renal artery stenosis", *Circulation*, Vol. 115, No. 2, pp. 263–269, Jan 2007.

76. *Renal Artery Stenting*, https://my.clevelandclinic.org/health/treatments/14868-renal-artery-stenting, Accessed Sep 2021.

77. Chan Yong Park, S. K. K., Soo Jin Na Choi, *Fracture of a Renal Artery Stent after PTAS in a Patient with Atherosclerotic Ostial Stenosis*, 2009, https://www.vsijournal.org/journal/view.html?spage=61&volume=25&number=1.

78. Miller, D. L., N. B. Smith, M. R. Bailey and et al, "Overview of Therapeutic Ultrasound Applications and Safety Considerations", *Journal of Ultrasound in Medicine*, Vol. 31, No. 4, pp. 623–634.

79. Oliveira, P., D. Pires-Oliveira, L. Bertin and et al, "The effect of therapeutic ultrasound on fibroblast cells in vitro: The systematic review", *Archivos de Medicina del Deporte*, Vol. 35, pp. 50–55, 01 2018.

80. Izadifar, Z., P. Babyn and D. Chapman, "Mechanical and Biological Effects of Ultrasound: A Review of Present Knowledge", *Ultrasound in Medicine & Biology*, Vol. 43, No. 6, pp. 1085–1104, 2017, https://www.sciencedirect.com/science/article/pii/S0301562917300522.

81. Domenici, F., C. Giliberti, A. Bedini and et al, "Structural and permeability sensitivity of cells to low intensity ultrasound: Infrared and fluorescence evidence in vitro", *Ultrasonics*, Vol. 54, No. 4, pp. 1020–1028, 2014, https://www.sciencedirect.com/science/article/pii/S0041624X13003417.

82. Murray, C. S. G., T. Nahar, H. Kalashyan and et al, "Ultrasound assessment of carotid arteries: Current concepts, methodologies, diagnostic criteria, and technological advancements", *Echocardiography*, Vol. 35, No. 12, pp. 2079–2091, 2018.

83. Clinics, M., *Carotid ultrasound*, https://www.mayoclinic.org/tests-procedures/carotid-ultrasound/about/pac-20393399, Accessed Sep 2021.

84. *Carotid Ultrasound*, https://vascularsurgery.ucsf.edu/conditions--procedures/carotid-ultrasound, Accessed Sep 2021.

85. Zhang, Y., H. Dong, Y. Xu and et al, "External Ultrasound for Carotid Atherosclerotic Plaque Treatment", *Journal of Ultrasound in Medicine*, Vol. 34, No. 3, pp. 451–459, 2015.

86. Wiegand, C., K. Bittenger, R. D. Galiano and et al, "Does noncontact low-frequency ultrasound therapy contribute to wound healing at the molecular level?", *Wound Repair and Regeneration*, Vol. 25, No. 5, pp. 871–882, 2017.

87. Driver, V. R., M. Yao and C. J. Miller, "Noncontact low-frequency ultrasound therapy in the treatment of chronic wounds: A meta-analysis", *Wound Repair and Regeneration*, Vol. 19, No. 4, pp. 475–480, 2011.

88. Korelo, R. I., M. Kryczyk, C. Garcia and et al, "Wound healing treatment by high frequency ultrasound, microcurrent, and combined therapy modifies the immune response in rats", *Braz J Phys Ther*, Vol. 20, No. 2, pp. 133–141, Jan 2016.

89. Franco de Oliveira, R., D. A. Pires Oliveira and C. P. Soares, "Effect of low-intensity pulsed ultrasound on l929 fibroblasts", *Arch Med Sci*, Vol. 7, No. 2, pp. 224–229, Apr 2011.

90. de Oliveira Perrucini, P. D., R. C. Poli-Frederico, D. A. de Almeida Pires-Oliveira and et al, "Anti-Inflammatory and Healing Effects of Pulsed Ultrasound Therapy on Fibroblasts", *Am J Phys Med Rehabil*, Vol. 99, No. 1, pp. 19–25, 01 2020.

91. Lai, J. and M. R. Pittelkow, "Physiological effects of ultrasound mist on fibroblasts", *International Journal of Dermatology*, Vol. 46, No. 6, pp. 587–593, 2007.

92. Bertin, L. D., R. C. Poli-Frederico, D. A. A. Pires Oliveira and et al, "Analysis of Cell Viability and Gene Expression After Continuous Ultrasound Therapy in L929 Fibroblast Cells", *Am J Phys Med Rehabil*, Vol. 98, No. 5, pp. 369–372, 05 2019.

93. Huang, J. J., Y. Q. Shi, R. L. Li and et al, "Angiogenesis effect of therapeutic ultrasound on ischemic hind limb in mice", *Am J Transl Res*, Vol. 6, No. 6, pp. 703–713, 2014.

94. Maxwell, L., "Therapeutic Ultrasound: Its Effects on the Cellular and Molecular Mechanisms of Inflammation and Repair", *Physiotherapy*, Vol. 78, No. 6, pp. 421–426, 1992, https://www.sciencedirect.com/science/article/pii/S0031940610615283.

95. Zhang, N., B. Xu, R. Xing and et al, "Low-intensity pulsed ultrasound inhibits IL-1β induced inflammation of fibroblast-like synoviosytes via NF-KB pathway", *Applied Acoustics*, Vol. 167, p. 107384, 10 2020.

96. Furusawa, Y., M. A. Hassan, Q.-L. Zhao and et al, "Effects of therapeutic ultrasound on the nucleus and genomic DNA", *Ultrasonics Sonochemistry*, Vol. 21, No. 6, pp. 2061–2068, 2014, https://www.sciencedirect.com/science/article/pii/S1350417714000777, aOSS 2013.

97. Doan, N., P. Reher, S. Meghji and et al, "In vitro effects of therapeutic ultrasound on cell proliferation, protein synthesis, and cytokine production by human fibroblasts, osteoblasts, and monocytes", *Journal of Oral and Maxillofacial Surgery*, Vol. 57, No. 4, pp. 409–419, 1999, https://www.sciencedirect.com/science/article/pii/S0278239199902811.

98. Mizrahi, N., D. Seliktar and E. Kimmel, "Ultrasound-Induced Angiogenic Response in Endothelial Cells", *Ultrasound in Medicine & Biology*, Vol. 33, No. 11, pp. 1818–1829, 2007, https://www.sciencedirect.com/science/article/pii/S0301562907002517.

99. Milowska, K. and T. Gabryelak, "Reactive oxygen species and DNA damage after ultrasound exposure", *Biomolecular Engineering*, Vol. 24, No. 2, pp. 263–267, 2007, https://www.sciencedirect.com/science/article/pii/S1389034407000226.

100. Feril, L. B. and T. Kondo, "Biological Effects of Low Intensity Ultrasound: The Mechanism Involved, and its Implications on Therapy and on Biosafety of Ultrasound", *Journal of Radiation Research*, Vol. 45, No. 4, pp. 479–489, 2004.

101. Jia, Y., W. Yuan, K. Zhang and et al, "Comparison of Cell Membrane Damage Induced by the Therapeutic Ultrasound on Human Breast Cancer MCF-7 and MCF-7/ADR Cells", *Ultrasonics Sonochemistry*, Vol. 26, pp. 128–135, 2015, https://www.sciencedirect.com/science/article/pii/S1350417715000516.

102. Mohd Bohari, S. P., H. Aboulkheyr, N. Johan and et al, "Low Intensity Ultrasound Induced Apoptosis in MCF-7 Breast Cancer Cell Lines", *Sains Malaysia*, Vol. 46, pp. 575–581, 04 2017.

103. Katiyar, A., J. Osborn, M. DasBanerjee and et al, "Inhibition of Human Breast Cancer Cell Proliferation by Low-Intensity Ultrasound Stimulation", *Journal of Ultrasound in Medicine*, Vol. 39, No. 10, pp. 2043–2052, 2020, https://onlinelibrary.wiley.com/doi/abs/10.1002/jum.15312.

104. Peek, M. C. L., M. Ahmed, A. Napoli, B. ten Haken, S. McWilliams, S. I. Usiskin, S. E. Pinder, M. van Hemelrijck and M. Douek, "Systematic review of high-intensity focused ultrasound ablation in the treatment of breast cancer", *British Journal of Surgery*, Vol. 102, No. 8, pp. 873–882, 06 2015, https://doi.org/10.1002/bjs.9793.

105. Şerban Comşa, M. R., Anca Maria Cimpean, "The Story of MCF-7 Breast Cancer Cell Line: 40 years of Experience in Research", *Anticancer Research*, Vol. 35, No. 6, pp. 3147–3154, 2015.

106. Feril, L. B., R. L. Fernan and K. Tachibana, "High-Intensity Focused Ultrasound in the Treatment of Breast Cancer", *Curr Med Chem*, Vol. 28, No. 25, pp. 5179–5188, 2021.

107. Wang, D., F. Peng, J. Li and et al, "Butyrate-inserted Ni–Ti layered double hydroxide film for H2O2-mediated tumor and bacteria killing", *Materials Today*, Vol. 20, No. 5, pp. 238–257, 2017, https://www.sciencedirect.com/science/article/pii/S1369702117300317.

108. Wu, F., Z. B. Wang, Y. D. Cao and et al, "A randomised clinical trial of high-intensity focused ultrasound ablation for the treatment of patients with localised breast cancer", *Br J Cancer*, Vol. 89, No. 12, pp. 2227–2233, Dec 2003.

109. *Technical Considerations for Non-Clinical Assessment of Medical Devices Containing Nitinol*, 2020.

110. Wirth, C., V. Comte, C. Lagneau and et al, "Nitinol surface roughness modulates in vitro cell response: a comparison between fibroblasts and osteoblasts",

Materials Science and Engineering: C, Vol. 25, No. 1, pp. 51–60, 2005, https://www.sciencedirect.com/science/article/pii/S0928493104000608.

111. S Miyazaki, Z. D., *Nitinol as a Biomedical Material*, 2016.

112. Ryhänen, J., E. Niemi, W. Serlo, E. Niemelä and et al, "Biocompatibility of nickel-titanium shape memory metal and its corrosion behavior in human cell cultures", *Journal of Biomedical Materials Research*, Vol. 35, No. 4, pp. 451–457, 1997.

113. Stoeckel, D., A. Pelton and T. Duerig, "Self-expanding nitinol stents: material and design considerations", *Eur Radiol*, Vol. 14, No. 2, pp. 292–301, Feb 2004.

114. Trepanier, C., R. Venugopalan, R. Messer and et al, "Effect of passivation treatments on nickel release from Nitinol", *Society for Biomateria.–6th World Biomaterials Congress, Transactions.*, Vol. 1043, 2000.

115. Bishara, S. E., R. D. Barrett and M. I. Selim, "Biodegradation of orthodontic appliances. Part II. Changes in the blood level of nickel", *American Journal of Orthodontics and Dentofacial Orthopedics*, Vol. 103, No. 2, pp. 115–119, 1993, https://www.sciencedirect.com/science/article/pii/S0889540605817603.

116. McGrath, D., B. OBrien, M. Bruzzi and et al, "Nitinol stent design – understanding axial buckling", *Journal of the Mechanical Behavior of Biomedical Materials*, Vol. 40, pp. 252–263, 2014, https://www.sciencedirect.com/science/article/pii/S1751616114002823.

117. Trépanier, C., T. K. Leung, M. Tabrizian and et al, "Preliminary investigation of the effects of surface treatments on biological response to shape memory NiTi stents", *Journal of Biomedical Materials Research*, Vol. 48, No. 2, pp. 165–171, 1999.

118. Chavalla, S., T. Hoffmann and D. Juhre, "Simulation of NiTi Stent Deployment in a Realistic Patient Carotid Artery Using Isogeometric Analysis", *Procedia Structural Integrity*, Vol. 15, pp. 8–15, 2019, https://www.sciencedirect.com/science/article/pii/S245232161930109X,

international Conference on Stents: Materials, Mechanics and Manufacturing ICS3M 2019.

119. Wu, W., M. Qi, X.-P. Liu and et al, "Delivery and release of nitinol stent in carotid artery and their interactions: A finite element analysis", *Journal of Biomechanics*, Vol. 40, No. 13, pp. 3034–3040, 2007.

120. Ahlhelm, F., R. Kaufmann, D. Ahlhelm and et al, "Carotid artery stenting using a novel self-expanding braided nickel-titanium stent: feasibility and safety porcine trial", *Cardiovasc Intervent Radiol*, Vol. 32, No. 5, pp. 1019–1027, Sep 2009.

121. *Roadsaver Carotid Artery Stent*, https://www.who.int/health-topics/cardiovasculardiseases#tabt̄ab_1/, Accessed Sep 2021.

122. Tatkare, D., *Stent Markets by Stents Type*, https://www.alliedmarketresearch.comstentsmarket, Accessed Sep 2021.

123. Rodrigues, R. O., D. Pinho, D. Bento and et al, "Wall expansion assessment of an intracranial aneurysm model by a 3D Digital Image Correlation System", *Measurement*, Vol. 88, pp. 262–270, 2016.

124. O'Brien, J., I. Wilson, T. Orton and et al, "Investigation of the Alamar Blue (resazurin) fluorescent dye for the assessment of mammalian cell cytotoxicity", *European Journal of Biochemistry*, Vol. 267, No. 17, pp. 5421–5426, 2000.

125. Byth, H.-A., B. I. Mchunu, I. A. Dubery and et al, "Assessment of a simple, non-toxic alamar blue cell survival assay to monitor tomato cell viability", *Phytochemical Analysis*, Vol. 12, No. 5, pp. 340–346, 2001.

126. Bank, H. L., *Rapid Assessment of Islet Viability with acridine Orange and Propidium Iodide*, 1998.

127. *Wikipedia contributors*, https://en.wikipedia.org/w/index.php?title=Immunofluorescenceoldid=1042082220, Online; accessed 6-October-2021.

128. Wikipedia, "Actin — Wikipedia, The Free Encyclopedia", https://en.wikipedia.org/wiki/Actin, 2021, [Online; accessed 30-September-2021].

129. *Actin staining techniques*, `https://www.cytoskeleton.com/actinstaining-techniques`, Accessed Sep 2021.

130. Tarnowski, B. I., F. G. Spinale and J. H. Nicholson, "DAPI as a Useful Stain for Nuclear Quantitation", *Biotechnic & Histochemistry*, Vol. 66, No. 6, pp. 296–302, 1991.

131. Dimmick, I., *The use of DAPI in multiple flow cytometry applications*, 2011.